الجـــــــــــــمـهـوريـــــة الجـــــــــزائـريـة الديمـــــــــقـراطيـة الـشـــــــــعـبيـة

PEOPLE'S DEMOCRATIC REPUBLIC OF ALGERIA

وزارة التـــــــــــــعـليـم العـــــالي والبـــــــــــحث العـــــلـمـــي

Ministry of Higher Education and Scientific Research

جامعة محمد البشير الإبراهيمي – برج بوعريريج

University of Mohamed El-Bachir El-Ibrahimi - Bordj Bou Arreridj

Faculty of Science and Technology

Department of Electromechanics

THÈSES

Presented for the award of the MASTER's degree

In: electrical engineering

Speciality: renewable energy in

Electrical engineering

BY: - Amari said

- Latrach islam

Subject

Comparative study of different MPPT control technique performances in photovoltaic system

Publicly supported, the 30 /06 /2025, before the jury composed of:

Mr. Slama Fateh	***Teacher.***	***Univ-BBA***	***President***
Mr. faleh Abdellah	***Teacher.***	**Univ-BBA**	***Supervisor***
Mr. Aissa Oualid	***MCA***	**Univ-BBA**	***Examiner***

University Year : 2024/2025

Acknowledgment

Praise be to Allah, by whose grace good deeds are completed and by whose guidance goals are achieved.

I would like to express my sincere thanks and deep appreciation to everyone who contributed to the completion of this thesis, especially:

Professor **faleh Abdellah**, my supervisor, for his continuous guidance, advice, and academic support. I am deeply grateful for the effort he put forth to help bring this work to its final form in the best way possible.

I would also like to extend my heartfelt thanks to all the professors who enriched my knowledge and opened for me new horizons of thought and research throughout the years of study.

My sincere gratitude goes to my beloved family, who were my first support and stood by me in all circumstances. I offer them my highest expressions of love and appreciation.

To everyone who lent me a helping hand, even with a kind word, I say: May Allah reward you all abundantly.

Dedication

To those who instilled in me values and nurtured my love for knowledge and learning...

To the heartbeat of my life, the light of my vision...

To my dear parents, symbols of sacrifice and generosity — I dedicate this success and the fruit of my efforts to you, in gratitude for your priceless support.

To my brothers and sisters, my pillars in life, who shared with me moments of struggle and joy...

To everyone who believed in me, encouraged me, and supported me — even with a kind word...

I dedicate this humble work to you, hoping to have lived up to your expectations.

Abstract

With the considerable increase in energy needs and the decrease in fossil energy resources in recent years, many countries in the world are interested in developing and increasing energy products through renewable energy, particularly photovoltaic energy. In this context, the present work aims to present a comparative study between two maximum power point tracking algorithms, namely Perturbed and Observed (P&O) and Incremental Conductance (INC), at a photovoltaic system. A comparative study of these two techniques was conducted using MATLAB/Simulink with a photovoltaic generator, a boost converter, and a resistive load. From the obtained results, the INC control generally provides better performance compared to the P&O control.

ملخص

مع الزيادة الكبيرة في احتياجات الطاقة وانخفاض موارد الطاقة الأحفورية في السنوات الأخيرة، اهتمت العديد من دول العالم بتطوير وزيادة منتجات الطاقة من خلال الطاقة المتجددة، وخاصةً الطاقة الكهروضوئية. في هذا السياق، يهدف هذا العمل إلى تقديم دراسة مقارنة بين خوارزميتين لتتبع نقطة القدرة القصوى، وهما: خوارزمية المضطربة والمرصودة (P&O)وخوارزمية الموصلية التزايدية(INC) ، في نظام كهروضوئي. أُجريت دراسة مقارنة لهاتين التقنيتين باستخدام MATLAB/Simulinkمع مولد كهروضوئي، ومحول تعزيز، وحمل مقاوم. بناءً على النتائج، يُظهر نظام التحكم INC أداءً أفضل مقارنةً بنظام التحكم.P&O

Résumé

Face à l'augmentation considérable des besoins énergétiques et à la diminution des ressources fossiles ces dernières années, de nombreux pays souhaitent développer et accroître leurs produits énergétiques grâce aux énergies renouvelables, notamment le photovoltaïque. Dans ce contexte, ce travail vise à présenter une étude comparative de deux algorithmes de suivi du point de puissance maximale, à savoir Perturbé et Observé (P&O) et Conductance Incrémentale (INC), sur un système photovoltaïque. Une étude comparative de ces deux techniques a été réalisée sous MATLAB/Simulink avec un générateur photovoltaïque, un convertisseur élévateur et une charge résistive. D'après les résultats obtenus, le contrôle INC offre généralement de meilleures performances que le contrôle P&O.

Summary

Tables

Figures

Symbols

R: Series resistance of the cell

Rsh: Shunt (parallel) resistance of the cell

Ipv: Current delivered by the cell

Iph: Photocurrent

Iphn: Nominal photocurrent

d: Diode

Id: Diode current

V_1 : Thermodynamic potential of the cell

I: Saturation current

K_1 : Temperature coefficient of short-circuit current (*Isc*)

Iscn: Nominal short-circuit current of the cell

Tref: Reference temperature of the PV cell [°C]

Voc: Open-circuit voltage

Pmax: Maximum power output of the PV cell [W]

Vmax: Voltage at maximum power point

Imax: Current at maximum power point

Vopt: Optimal voltage

Iopt: Optimal current

n: Diode ideality factor

Vpv: Output voltage of the PV cell

Gref: Reference irradiance (1000 W/m²)

K: Temperature coefficient of open-circuit voltage (*Voc*)

Id_1 : Current through the first diode

Id_2 : Current through the second diode

Io_1 : Saturation current of the first diode

Io_2 : Saturation current of the second diode

L: Input inductance of the chopper

C_1 : Input capacitance of the chopper

C_2 : Output capacitance of the chopper

D: Duty cycle

Ts: Switching period of the chopper

fs: Switching frequency of the chopper

VL: Voltage across the inductor

Vde: Output voltage of the chopper

Ipv: Input current to the chopper

$$\mathbf{e = I + V\left(\frac{\Delta Ipv}{\Delta Vpv}\right)}$$

List of Acronyms

PV: Photovoltaic

GPV: Photovoltaic Generator

IGBT: Insulated Gate Bipolar Transistor

VCO: Voltage Controlled Oscillator

PID (corrected from ID): Proportional-Integral-Derivative Controller

LV (corrected from V): Low Voltage

PWM: Pulse Width Modulation

MPPT: Maximum Power Point Tracking

MPP (corrected from PPM): Maximum Power Point

P&O : Perturb and Observe

INC : Incremental Conductance

DC : Direct Current

DC/DC: Direct Current to Direct Current (converter)

P : Active Power

Ns: Number of cells in series

Np: Number of cells in parallel

General Introduction

General Introduction

Electricity is currently the easiest form of energy to exploit. But before it can be consumed, it must be produced, generally in high-power production units, transported, and then distributed to each consumer. In industrialized countries, this system is now highly centralized. [1]

Energy production is a major challenge for the coming years. Indeed, the energy needs of industrialized societies are constantly increasing. Furthermore, developing countries will need more and more energy to pursue their development. Today, a large portion of global energy production is provided by fossil fuels. The consumption of these sources results in greenhouse gas emissions and therefore an increase in pollution. The additional danger is that excessive consumption of natural resources will uncontrollably reduce reserves of this type of energy for future generations. [2]

There are two types of energy: non-renewable energy and renewable energy. The former are derived from oil, gas, coal, and uranium. The latter are derived from hydropower, biomass, waste, wind, solar, geothermal, etc. [3]

In this general context, our study focuses on the photovoltaic (PV) sector, which appears to be one of the most promising, with a very high global growth rate.

PV energy is obtained directly from the sun's rays. It can even be transformed into electrical energy thanks to the photovoltaic effect. PV panels composed of PV cells have the ability to transform photons into electrons. The energy, in the form of direct current, is therefore directly usable. [4-5]

Due to the highly nonlinear electrical characteristics of PV cells and their combinations, the efficiency of PV systems can be improved by solutions using maximum power point tracking (MPPT) techniques.

In this work, we focused primarily on developing an optimization procedure that enables Maximum Power Point Tracking (MPPT) of a photovoltaic generator (PVG), for efficient operation of the PV array. Indeed, for example, in the case of mobile vehicles powered by photovoltaic energy, power must be ensured at the Maximum Power Point Tracking (MPPT) regardless of weather conditions (temperature and irradiation). This requires the implementation of a Maximum Power Point Tracking (MPPT) technique, such as the Perturbation-Observation (P&O) and Incremental conductance (IncCond) method. [6-7]

The presented work is organized into three chapters

- Chapter I presents an overview of photovoltaic systems.
- Next, we will move on to the second chapter, firstly, we will also discuss some techniques of maximum power point tracking (MPPT), and we will explore the "Perturbation-Observation" and" Incremental conductance" methods. Secondly, we will present three types of DC-DC converters: boost, buck and buck-boost converters.
- Finally, the third chapter, it will be completed by a comparative study between the so-called conventional methods, namely the Perturbation-Observation (P&O) and Incremental conductance (IncCond.) method,

The results obtained highlight the Perturbation and Observation (P&O) and IncCond methods

Chapter I: General Information on Photovoltaic Systems

Chapitre I : general information on photovoltaic systems

I.1. Introduction

Photovoltaic solar energy is a renewable energy source produced by the sun's rays. **It** is one of the most important sources of renewable energy, and many countries have been increasingly interested in it in recent years.

In this chapter, we will present:

- Photovoltaic generator
- Photovoltaic effect
- Photovoltaic (PV) cell :
  - Photovoltaic cell operating principle
  - Photovoltaic cell assembly
  - Photovoltaic cell technology
  - Photovoltaic Cell Modeling
- Types of PV systems :
  - Stand-alone PV System
  - Direct-Coupled PV System
  - Hybrid PV System
  - Grid-connected PV system

I.2. Photovoltaic generator

The main component of a PV generator is the photovoltaic cell. Typically, it measures a few square centimeter's and produces approximately 1 W to 3 W of power. To achieve high power, several modules connected mechanically and electrically form a panel, a common structure that can be mounted on the ground or a building. Several panels electrically connected in series form a row, and several rows electrically connected in parallel to generate the required energy constitute the generator or photovoltaic field [8]

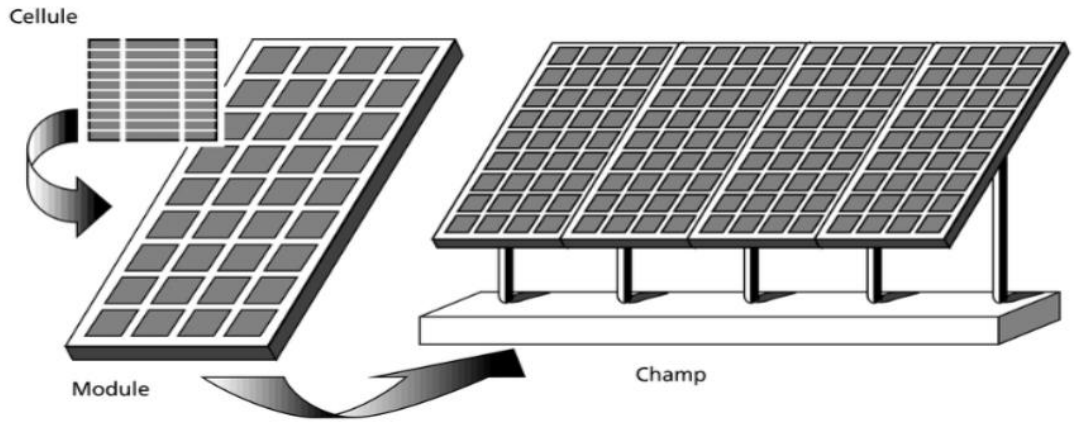

Figure I-1-: Photovotaic generator

I.3. Photovoltaic Effect

The transformation of solar energy into electricity is based on the photovoltaic effect, which is the ability of photons to generate charge carriers (electrons and holes) in a material. When a semiconductor is exposed to radiation of the appropriate wavelength (the photon energy must be at least equivalent to that of the material's band gap), the energy absorbed by the photons promotes electronic transitions from the valence band to the conduction band of the semiconductor. This produces electron-hole pairs that can participate in current transport (photoconductivity) when the material is polarized [9].

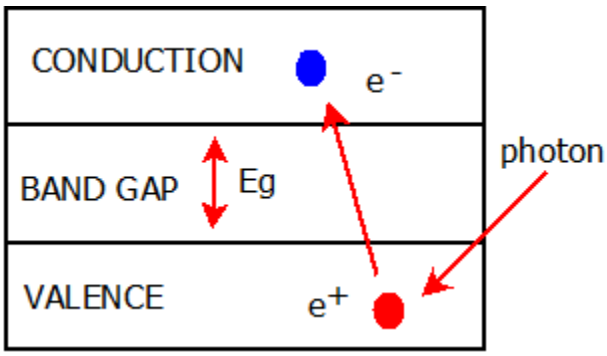

Figure I- 2: Photovoltaic effect in a solar cell

I.4. Photovoltaic (PV) cell

A photovoltaic cell is based on the physical phenomenon called the photovoltaic effect, which consists of establishing an electromotive force when the surface of this cell is exposed to light (Figure I-3). The voltage generated can vary between 0.3 V and 0.7 V depending on the material used and its arrangement as well as the temperature of the cell and the aging of the cell [10].

Figure I- 3: Photovoltaic cell

I.4.1. Photovoltaic cell operating principle

A PV cell is made from two layers of silicon, one P-doped (boron-doped) and the other N-doped (phosphorus-doped), creating a PN junction with a potential barrier see (Figure I-4). When photons are absorbed by the semiconductor, they transfer their energy to the atoms of the PN junction so that the electrons in these atoms are released and create electrons (N charges) and holes (P charges). This then creates a potential difference between the two layers. This potential difference is measurable between the connections of the positive and negative terminals of the cell. Through continuous charging, carriers can also be collected. The maximum voltage of the cell is about 0.6 V for zero current. This voltage is called the

open circuit voltage (OCV). The maximum current occurs when the cell terminals are short-circuited, it is called short-circuit current (Isc) and is highly dependent on the illumination level [11].

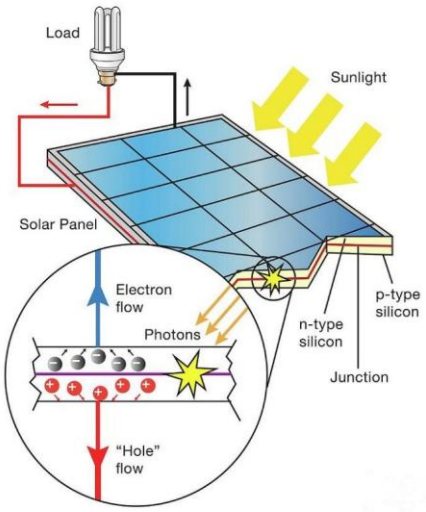

Figure I- 4: Photovoltaic cell operating principle

I.4.2. Photovoltaic cell assembly

The single photovoltaic cell produces very low power between 1W to 3W with a voltage of less than one volt, which is not sufficient to meet the needs of electrical equipment, so it is assembled to give the desired power. There are three assembly types [12].

a Series assembly

Series connection allows the voltage to be increased by collecting the voltage from each cell, but the current remains the same for a cell as seen by (Figure I-.5) [12].

With the relationship:

$$Voc_{Ns} = Ns * Voc \quad (I.1)$$

$$Isc = Isc_{Ns} \quad (1.2)$$

V_{ocNs}: Sum of open circuit voltages
I_{scNs}: Short circuit current of cells in series.
Ns: Cells number in series.

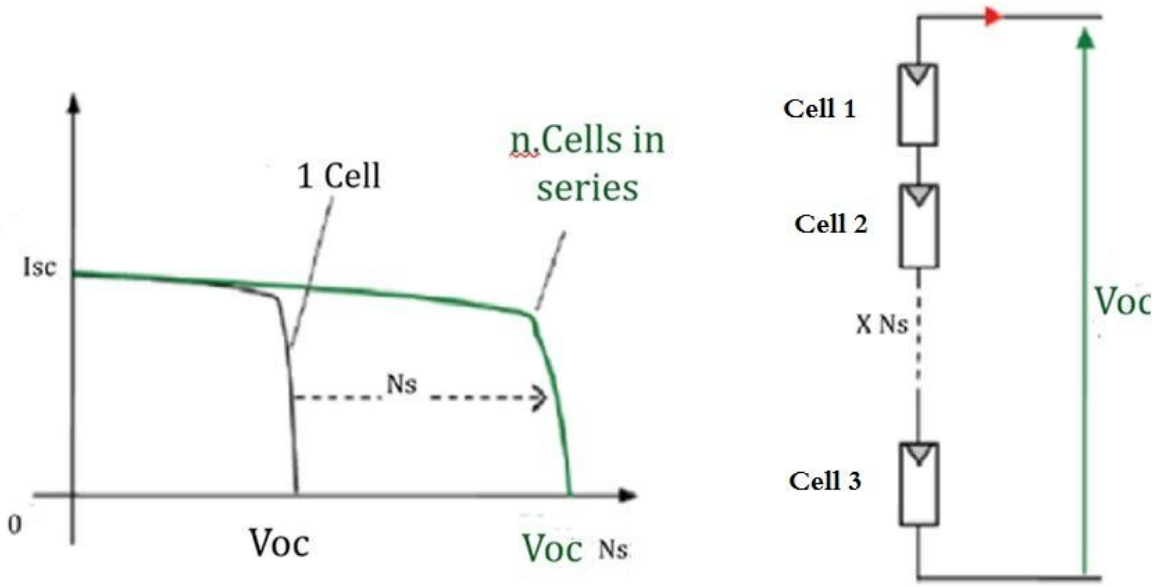

Figure I-5: Characteristic representation of current and voltage in the case of a series connection of cells

b.Parallel assembly

Parallel connection increases the current by collecting the current from each cell, but the voltage remains the same for a cell [12].

With the relationship:

$$Isc_{Np} = Np \times Isc \quad \text{(I.3)}$$

$$Voc = Voc_{Np} \quad \text{(I.4)}$$

I_{scNp} : Sums of short-circuit currents in case of cell parallel connection.
V_{ocNp}: Open circuit voltage of cells in case of parallel connection.
Np: Number of cells in parallel.

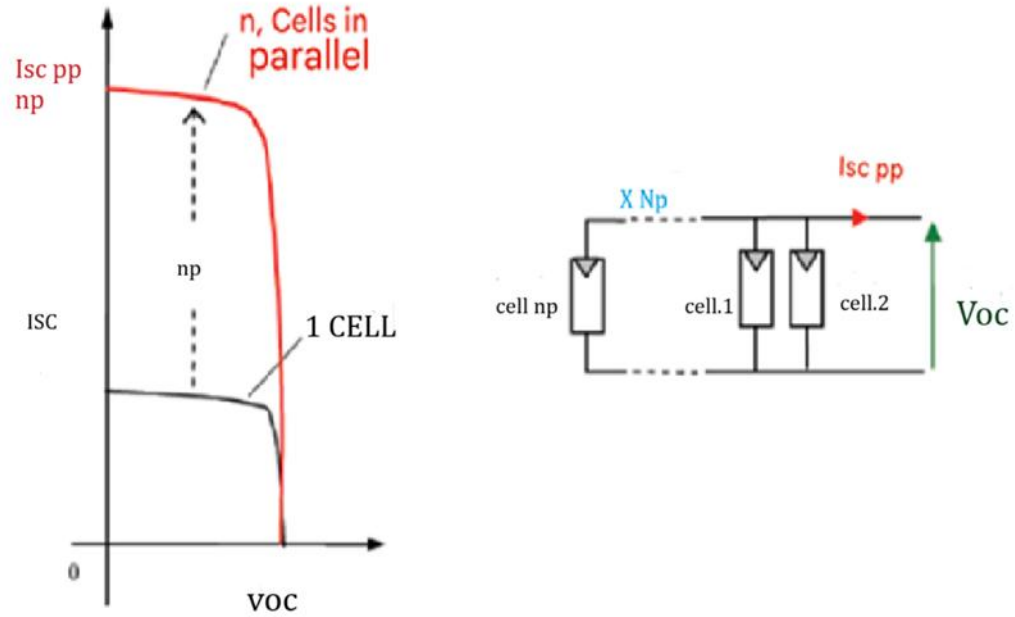

Figure I- 6: Characteristic representation of current and voltage in the case of a parallel connection of cells

c.Series-parallel assembly

To increase the voltage and current together, the cells must be connected in series-parallel [12].
The figure shows the series-parallel connection of the cells.
With the relationship:

$$Isc_{Np} = Np \times Isc \quad \text{(I.5)}$$

$$Voc_{Ns} = Ns * Voc \quad \text{(I.6)}$$

I_{scNp} : Sums of parallel short-circuit currents.
V_{ocNs}: Sum of open-circuit voltages.
Np: Number of cells in parallel.
Ns: Number of cells in series.

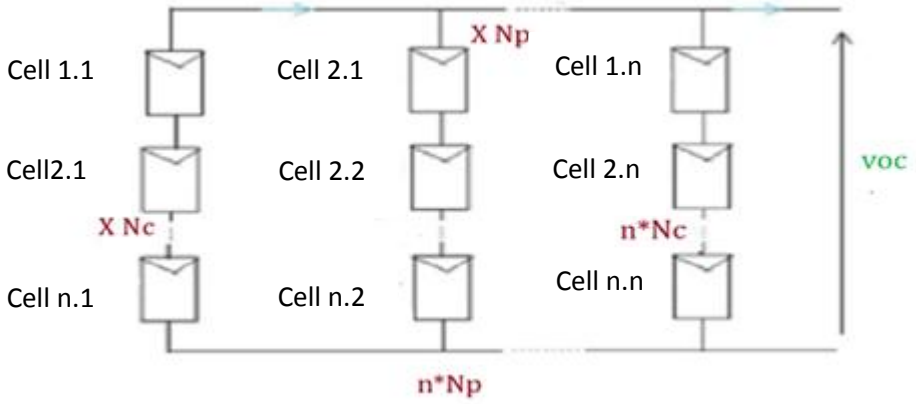

Figure I- 7: Series-parallel assembly of cells

I.4.3. Photovoltaic cell technology

Photovoltaic solar cells made from silicon are the most widely commercialized technology. Other technologies are also used, such as gallium arsenide (GaAs), which is characterized by better electrical power generation than silicon. However, this type of material is rare and expensive, and it is generally used in space applications due to its high efficiency. Furthermore, other less widely used materials exist, such as cadmium telluride (CdTe), cadmium diselenide, germanium (Ge), selenium (Se), and copper indium (commonly known as CIS).

There are a large number of industrialized technologies that implement the photovoltaic effect. Many are still in the research and development phase. The main technologies available on the market are:

- Crystalline silicon (monocrystalline and multicrystalline).
- Thin film **solar cell** [13].

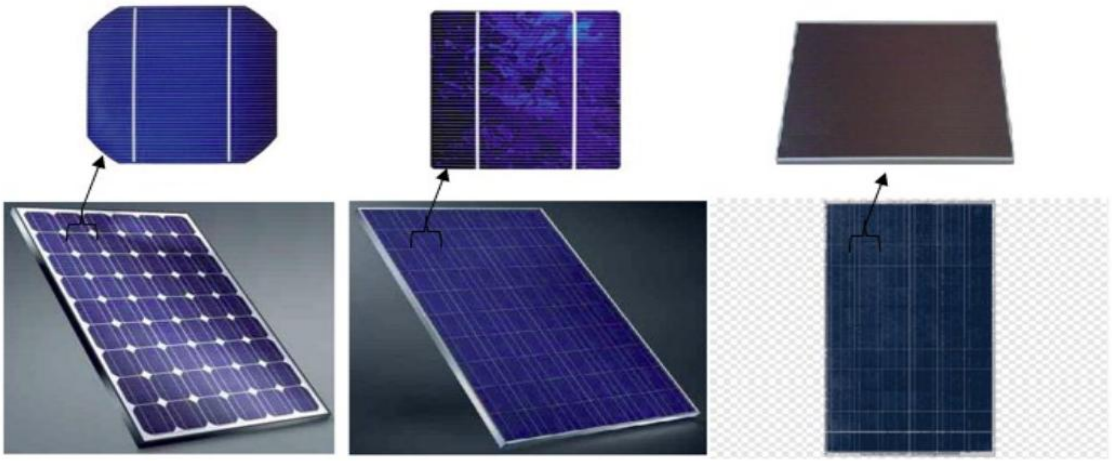

Monocrystalline **Polycrystalline** **Thin-film solar cell**

Figure I- 8: Silicon wafer

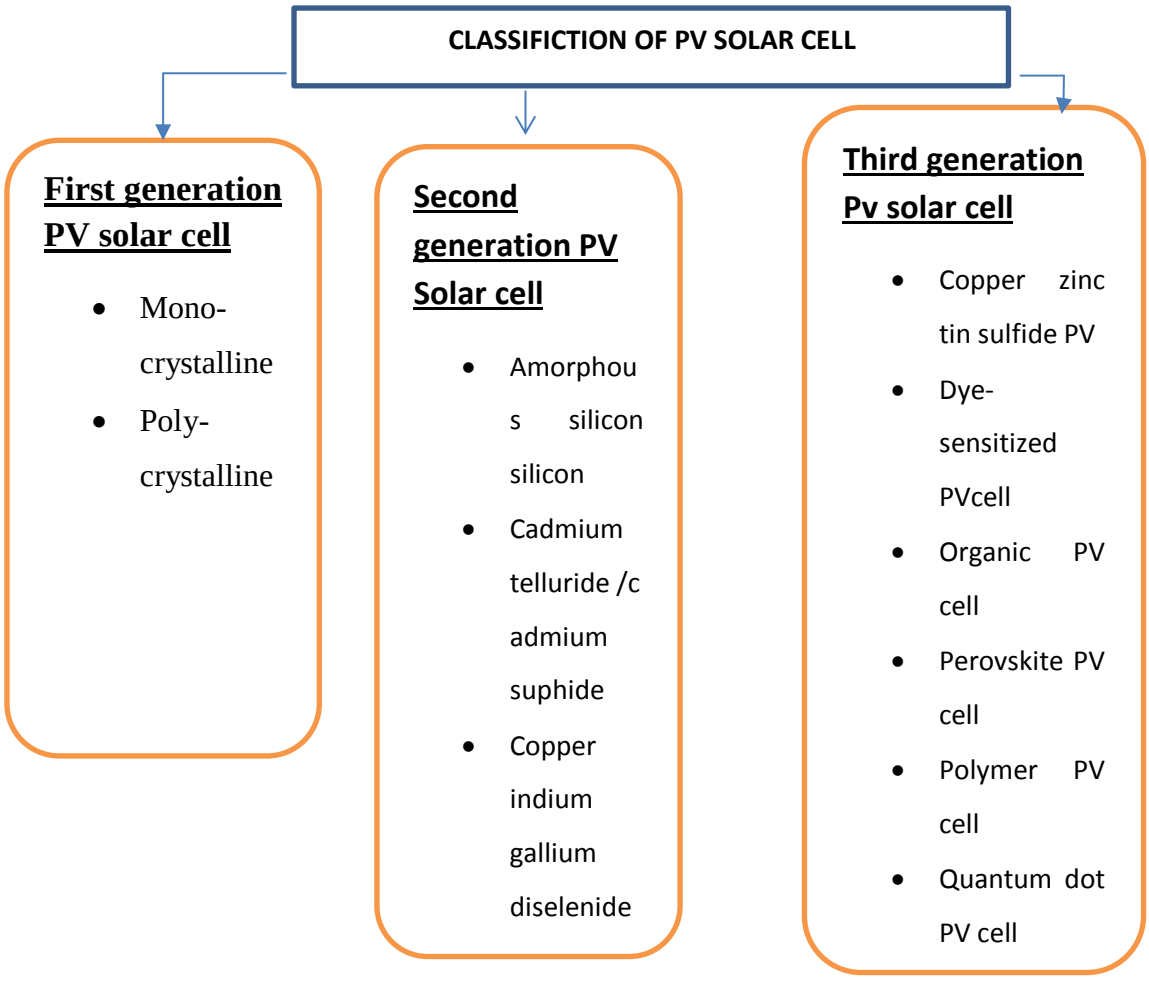

Figure I- 9: Classification of solar PV cell

Photovoltaic technologies can be classified into three main generations see the (Figure I.9.):

1- First-generation photovoltaic cells, which are Silicon based PV cells including monocrystalline and polycrystalline Silicon.
2- Second generation photovoltaic cells, including thin-film PV cells such as amorphous (a-Si), copper indium gallium diselenide (CIGS) and cadmium telluride/cadmium sulphide (CdTe/CdS), which aims to use less material whilst preserve the efficiencies of first PV cell generation.
3- Third generation photovoltaic cells, including copper zinc tin sulfide (CZTS), a dyesensitized solar cell (DSSC), organic, perovskite, polymer and quantum dot PV cells, which aims to reach high efficiencies but still use thin film second-generation deposition techniques.[14].

Table 1.1 presents a comparison between different PV module technologies in terms of efficiency and lifetime.

Table 1: Comparison between different PV Module Technologies [13]

Technology	Conversion yield	Lifetime
Polycrystalline silicon	12 to 16% (industrial)	35 years
Monocrystalline silicon	15 to 20% (industrial)	3515 to 20% (industrial)
Thin film amorphous silicon	7% (industrial)	< 10 years (en xtérieur)
CIS thin layer	10 to 12% (laboratory)	Not rated
Organic/inorganic sector	3 à 5 %	A few months

I.4.4. Photovoltaic Cell Modeling

There are several electrical models characterizing the operation of a photovoltaic cell, and they all have the common factor of considering the PV cell. PV panel are the basic elements of any photovoltaic system. They can be connected in series to increase their operating voltage and in parallel to increase their current. This assembly is called the photovoltaic generator as an ideal current generator.

In this work we will present three models of the following PV cell [15]:

a. Ideal Model

b. Real Model with One Diode

c. Real Model with Two Diodes

a. Ideal Model

In this model, the solar cell consists of an ideal current source generating a current I_{ph} proportional to the incident light power, in parallel with a diode that represents the PN transition area of …. the photovoltaic cell [16].

Figure I.10 illustrates the equivalent electrical diagram of this model:

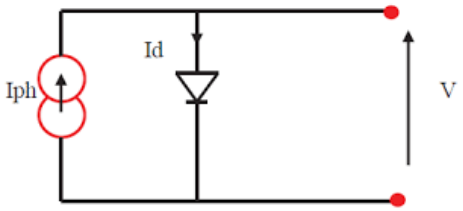

Figure I- 10: Equivalent circuit of the ideal model of a PV cell

The characteristic equation of this model is deduced in a direct manner from Kirchhoff's law [9]

$$I = I_{ph} - I_d \quad \text{(I.7)}$$

The diode being a non-linear element, its I-V characteristic is given by the relation:

$$I_d = I_s\left(e^{v_d/v_{th}} - 1\right) \quad \text{(I.8)}$$

SO:

$$I_d = I_{ph} - I_s((e^{\left(v_d/A\right)}) * v_{th} - 1)), \quad \text{(I.9)}$$

Where:

I_{ph} : is the photocurrent;
A: is the diode's ideality factor;
I_s: Diode saturation current given by:

$$I_s = K_1 T_3 e - V_g KT \quad \text{(I.10)}$$

V_{th}: Thermal voltage at temperature:

$$V_{th} = KT_q \quad \text{(I.11)}$$

With:
q: electron charge (1.602×10-19 C),

K: Boltzmann constant (1.381×10-23 J/k) K1: constant (1.2 A/cm2 K3)

T: effective cell temperature in Kelvin

V_g: gap energy (for crystalline silicon it is equal to 1.12 eV)

b. Real Single-Diode Model

This model is the most used in many researches thanks to its behavior which is closer to a PV cell compared to the ideal model on the one hand, and its simplicity for mathematical calculation compared to other models like the two-diode model on the other hand

In this model the PV cell is represented as a current source producing the photocurrent **I_{ph}**, models the conversion of the irradiation flux into electrical energy, mounted in parallel with a diode which models the PN junction. To optimize the modeling of some phenomena at the cell level, this model as shown in (Figure I-11) contains a series resistance R_s models the ohmic losses of the material and a shunt resistance R_{sh} models the parasitic currents which pass through the cell [17].

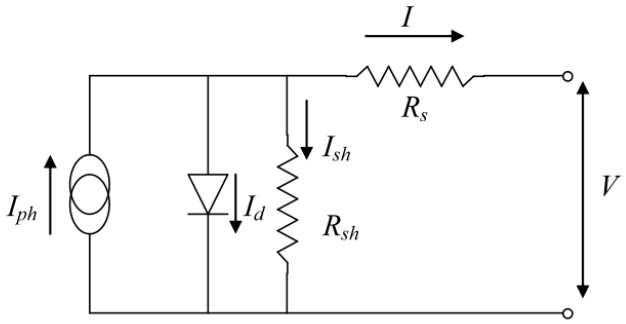

Figure I- 11: Equivalent circuit of the real model with a diode

The current generated by this model is given by [16]:

$$I = I_{ph} - I_d - I_{R_{sh}} \quad \text{(I.12)}$$

$$I_{R_{sh}} = \frac{V_d}{R_{sh}} \quad \text{(I.13)}$$

$$V_d = U + R_s I \quad \text{(I.14)}$$

The electric current produced by the cell is then given by the following expression:

$$I = I_{ph} - I_s\left(e^{\frac{(U+R_S I)}{A} \times V_{th}} - 1\right) \quad \text{(I.15)}$$

c- Two-Diode Model

This model differs from the previous one in that it includes two diodes. One models diffusion losses in the junction, while the other models recombination losses [17]. The equivalent electrical circuit is shown in the figure below:

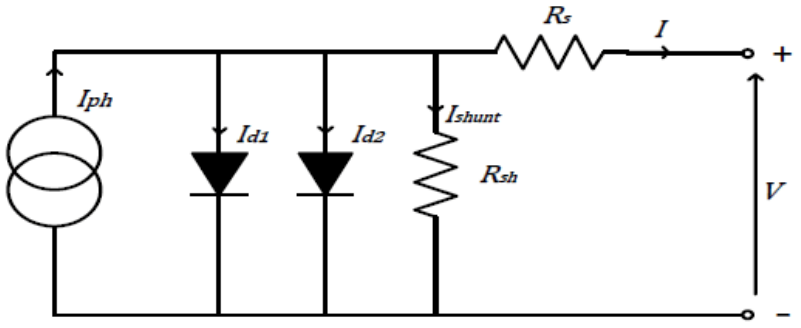

Figure I- 12: Equivalent circuit of the two-diode model

This model translates to the following electrical equation:

$$I = I_{Ph} - I_{d_1} - I_{d_2} - I_{R_{sh}} \quad \text{(I.16)}$$

The diode currents are given by:

$$I_{d_1} = I_{O_1}\left(e^{\frac{v_{pv} - R_S I_{pv}}{n_1 V_t}} - 1\right) \quad \text{(I.17)}$$

$$I_{d_2} = I_{O_2}\left(e^{\frac{v_{pv} - R_S I_{pv}}{n_2 V_t}} - 1\right) \quad \text{(I.18)}$$

$I_{O_1} = I_{O_2}$: saturation currents of the diode

n_1 ; n_2 : ideality factors (usually $n_1 \approx 1$, $n_2 \approx 2$)

I.5. Types of PV Systems

The selection of the type of photovoltaic system is particularly linked to the intended use and installation sites. There are generally four main categories of photovoltaic systems:

I.5.1. Stand-alone PV System

This system is frequently used in locations that are difficult to access or without a connection to the electrical grid. Called stand-alone, they rely primarily on exposure to sunlight to generate energy, without requiring an external connection or power supply [18].

They may also rely on the power grid or rely on some form of cogeneration. However, batteries are essential to maintain a constant electrical current, which is why lead-sulfuric acid batteries remain the most commonly used. The energy generated in direct current will be used directly when there is sunlight and will also be stored in batteries when excess energy is present. These batteries promptly guarantee the production of energy in the event of a shortage or absence of sunlight [18].

Consisting of a storage system and a packaging unit, it includes a charge controller, an MPPT (maximum power point tracking) device, and sometimes an inverter to convert the DC electricity produced into AC electricity needed for AC loads.

A standard stand-alone photovoltaic system is illustrated in Figure I.13 [18].

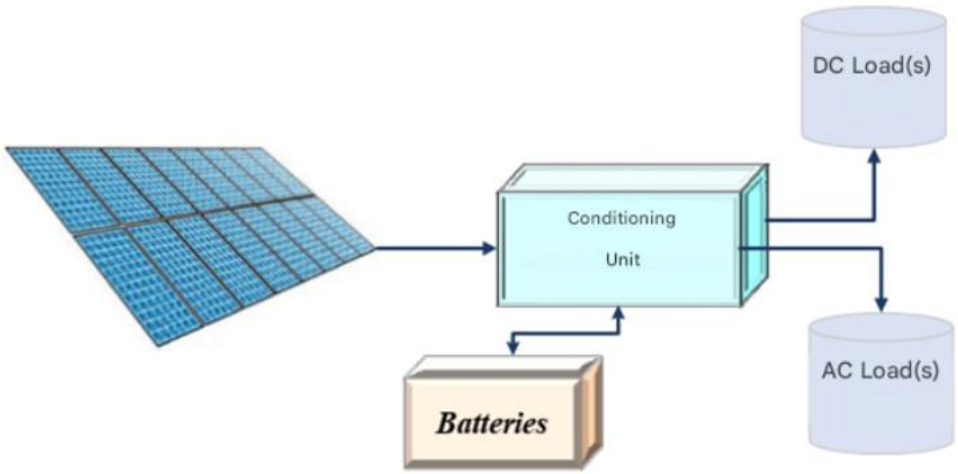

Figure I- 13: Stand-alone PV system

I.5.2. Direct-Coupled PV System

In a direct-coupled PV system, the PV generator is connected directly to a DC or AC load(s). Therefore, the load can only operate when solar irradiation is present; such a PV system is used only in limited applications. The typical application of this type of system is water pumping, where the PV generator operates to power the water pump motor, as shown in Figure (I-14). Note that in this case, the conditioning unit contains a motor with an appropriate static converter stage.[18]

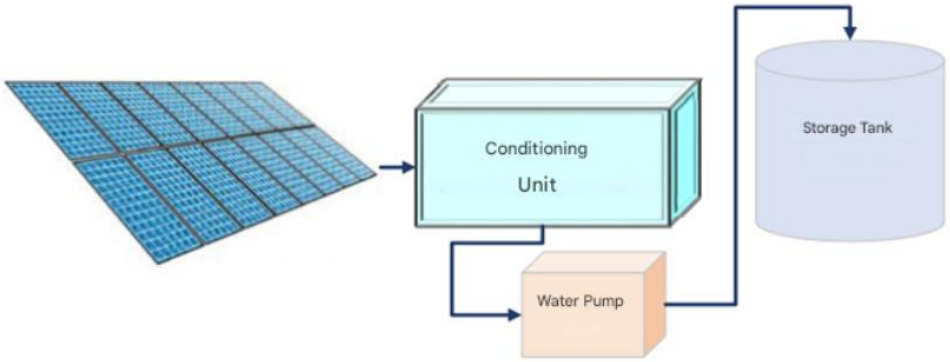

Figure I- 14: PV system powering a water pump

I.5.3. Hybrid PV System

This type is currently widespread; it involves integrating other generators with the PV system, as shown in (Figure I-15). The associated generator can be renewable, such as a wind turbine, conventional turbine, or diesel generator powered by biofuels, or non-renewable, such as a diesel engine or the electrical distribution grid. It is even possible to integrate a thermal system to heat domestic water or provide air conditioning by exploiting the heat dissipated by the PV system.

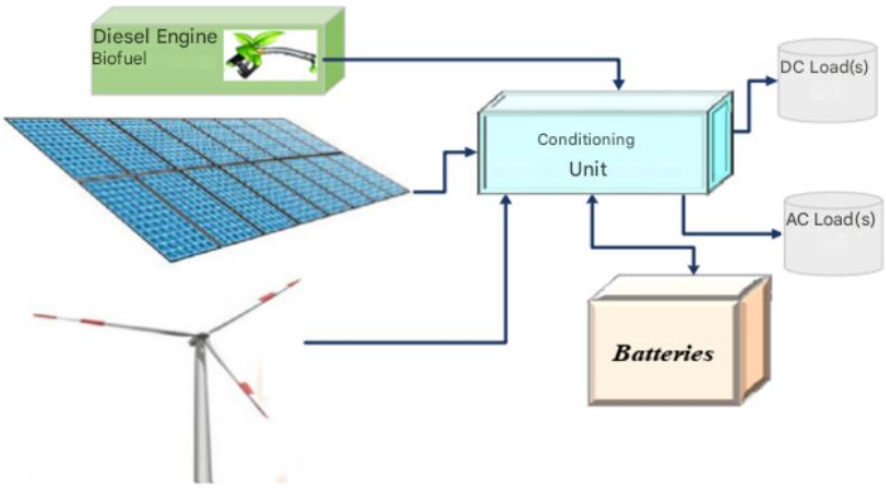

Figure I-15: Hybrid PV system

I.5.4. Grid-connected PV system

This is the most widely installed type of PV system; at the end of 2009, 95% of PV systems installed in France and 99% in Japan were grid-connected.

This system essentially consists of an inverter designed to convert DC/AC power fed into the grid, and an MPPT system associated with a DC/DC converter sized according to energy needs, as illustrated in (Figure I-16).

During periods when sunlight is available, the energy generated by this photovoltaic system can be used directly (as is common for PV systems integrated into commercial buildings and industrial applications) or sold to a company [18].

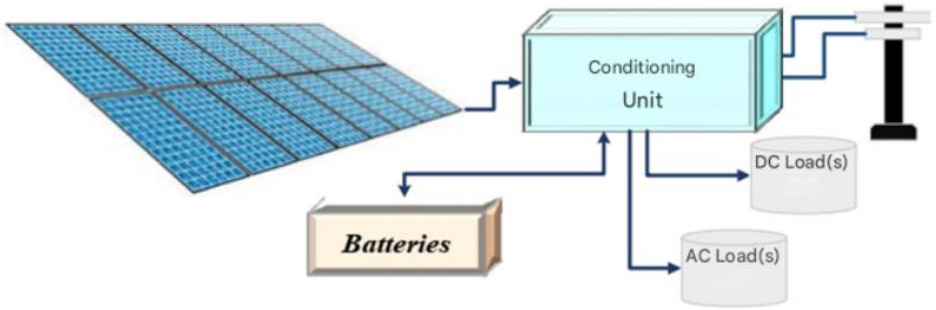

Figure I- 16: Grid-connected PV system

I.6. Conclusion

This chapter focused on introducing the photovoltaic generator and give general information about different elements of photovoltaic generator (cells, panel, mathematical modeling of PV cell). Also, we present the different type of photovoltaic systems, with their operating principles.

In the next chapter, we will discuss the basic MPPT controller with different DC -DC converters.

Chapter II:

Different Methods of Maximum Power Point Tracking with DC-DC Photovoltaic Converters

Chapter II: Different Methods of Maximum Power Point Tracking with DC-DC Photovoltaic Converters

II.1 Introduction

Maximum Power Point Tracking (MPPT) is a control method used in photovoltaic systems to track and maintain the solar array's operation at its maximum power point, regardless of environmental conditions (sunlight, temperature, etc.).

In this chapter, we first introduce traditional MPPT (P&O_INC_FCC_FCO), as well as DC-DC photovoltaic converters designed for photovoltaic systems

2.2. Maximum Power Point Tracking (MPPT)

MPPT control is a method that allows the PV generator to work at its maximum power regardless of the weather conditions of irradiation and temperature. The principle of this control as shown in figure (II.1) is based on the automatic variation of the duty cycle D of a DC-DC converter to the appropriate value in order to continuously maximize the power at the output of the PV panel.

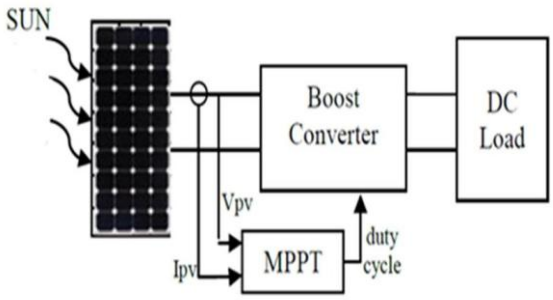

Figure II- 1: MPPT control block of PV system

II.1 Indirect methods:

This type of MPPT controls uses the existing link between the measured variables (Isc or Voc), which can be easily determined, and the approximate position of the MPP. It also includes controls based on an estimation of the operating point of the photovoltaic generator (GPV) made from a previously defined parametric model. Among these methods, we find the open circuit voltage method of the generator (Voc) voltage fraction algorithm), the short circuit method (Isc) current fraction algorithm) [19]:

II.1.1 Fractional Voltage Coefficient (FCO) Algorithm

This MPPT search technique consists of comparing the panel voltage Vpv with a reference voltage that corresponds to the optimal voltage Vmpp (figure II.2). The voltage error is then used to adjust the converter duty cycle. The reference voltage is obtained from the knowledge of the existing linear relationship between Vmpp and Voc of a PV module:

$$V_{mpp} = k_v * V_{OC} \quad \text{(II.1)}$$

Where kv is a voltage factor depending on the characteristics of the PV cell and which varies between 0.73 and 0.8.

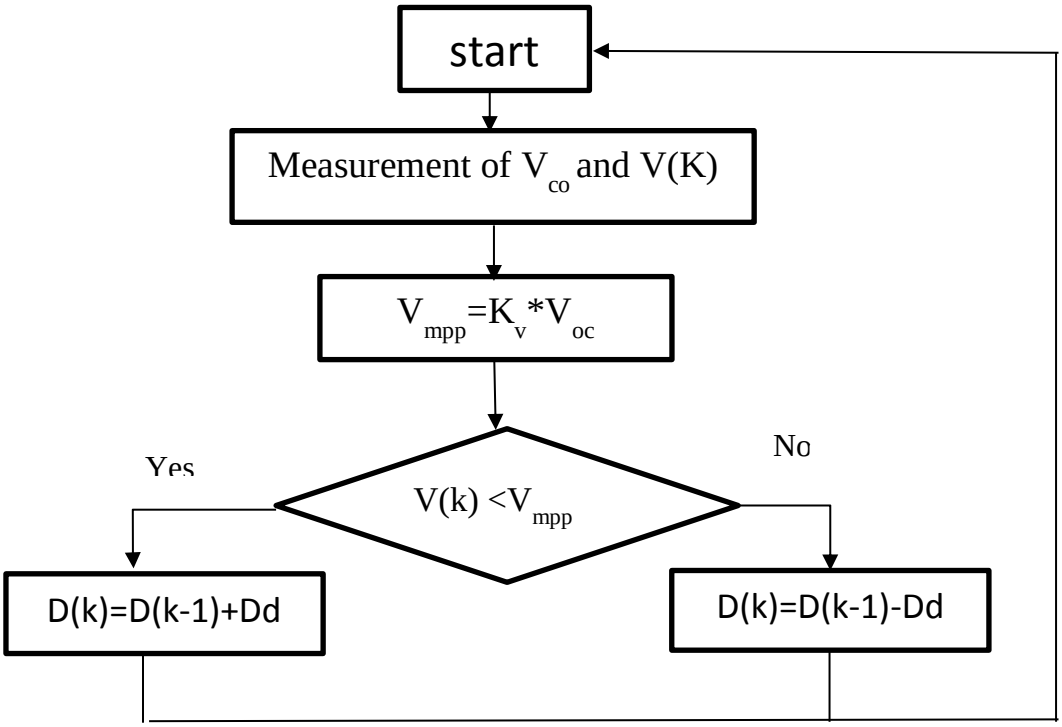

Figure II-2: Flowchart of the FCO algorithm

To deduce the optimal voltage, the open circuit voltage Vco must be measured. Therefore, the operating point of the panel is kept close to the optimal point by adjusting the panel voltage to the calculated optimal voltage. The process allows cyclically acting on the duty cycle to reach the optimal voltage. The major drawback of this technique lies in the need to measure Vco from time to time and the obligation to disconnect the load from the PV panel during this measurement, implying a loss of power transfer at each measurement. [20] [21]

II.1.2 Fractional Current Calculation (FCC) algorithm Isc

This technique is based on the linear relationship between the short-circuit current and the optimal current (Figure II.3) given by the following equation:

$$\boldsymbol{I_{mpp} = k_i * I_{sc}} \qquad \textit{(II.2)}$$

Where, k_i is a current factor depending on the characteristics of the PV cell and which varies between 0.85 and 0.92.

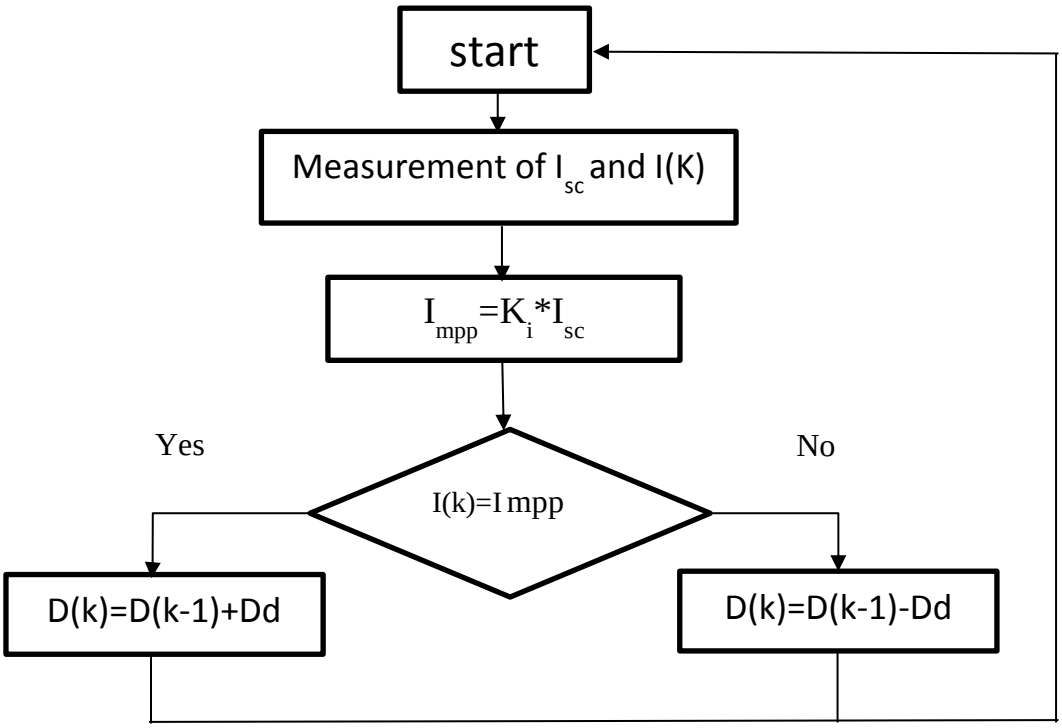

Figure II-3: Flowchart of the FCC algorithm

Indeed, the MPPT is obtained by bringing the panel current to the optimal current. Equation (II.2) shows that the Impp current can be determined by an Isc measurement. The Isc measurement involves a loss of power transfer due to the short-circuiting of the GPV. However, this method can be more accurate than the previous one because the temperature does not influence this coefficient too much.[20] [21]

II.2 Direct methods

This type of MPPT control determines the optimal operating point (MPP) from the currents, voltages or powers measured in the system. It can therefore react to unpredictable changes in the GPV operation. Generally, these procedures are based on search algorithms, with which the maximum power point is determined without interruption of operation. Among the direct algorithms of maximum power point searches are:[22]

- Perturb and observe (P&O) algorithm
- Conductance Increment (INC) Algorithm
- Hill Climbing Algorithm
- Smart MPPT controllers based on: fuzzy logic principle (FLC), artificial neural networks (ANN), …

II.2.1 Perturb and observe (P&O) algorithm

The principle of this method consists of disturbing, with a low amplitude, the output voltage of the GPV and then observing the behavior of the variation of the power at its output as shown in the following figure:[23]

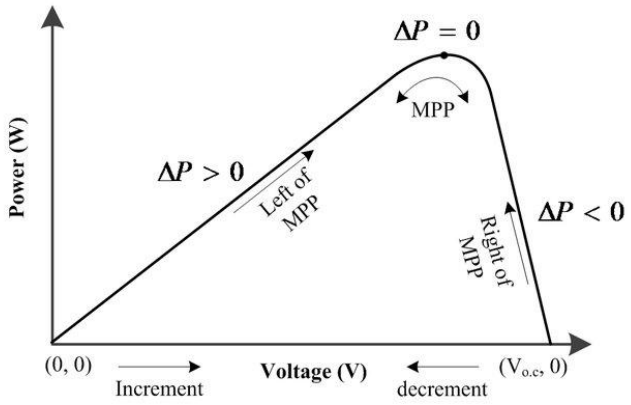

Figure II-4: Principle of the P&O method [24]

Depending on this variation, the algorithm decides to increment or decrement the GPV output voltage during the next iteration. From this figure, we can deduce that if a positive increment of V ($\Delta V > 0$) results in an increase of P ($\Delta P > 0$) then the operating point has not yet reached the MPPT. Otherwise ($\Delta V > 0$ and $\Delta P < 0$), this means that the operating point has exceeded the MPPT. A similar reasoning can be carried out when the voltage decreases ($\Delta V < 0$). In summary, when ΔP is positive following a disturbance on V, then the direction of disturbance must be maintained. Otherwise, the disturbance is reversed in order to resume convergence towards the MPPT.

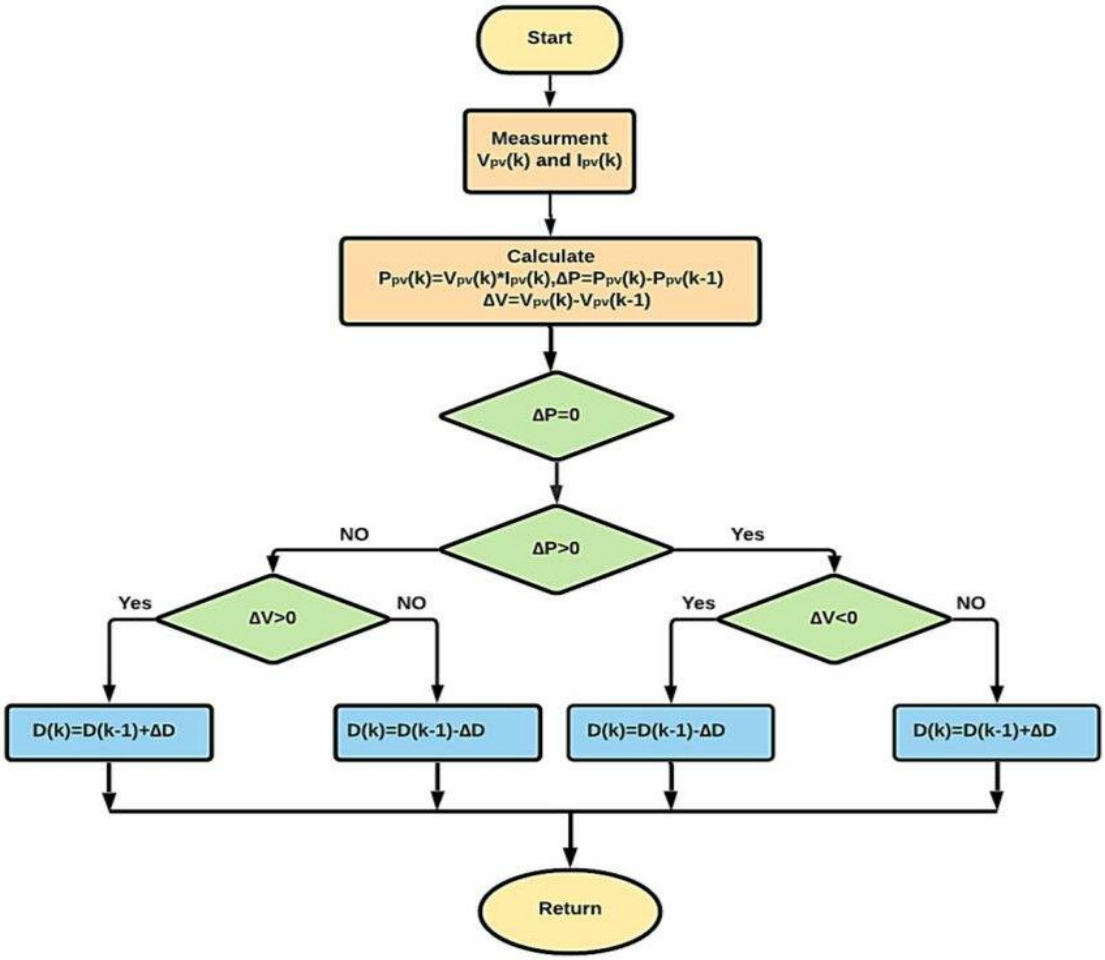

Figure II-5: flowchart P&O algorithm

Due to its simplicity of implementation, the P&O algorithm is widely used today. However, it has some problems related to its lack of precision. On the one hand, faced with a rapid variation of solar irradiance, the P&O algorithm does not correctly track the PPM. On the other hand, the major drawback of this algorithm is its oscillatory behavior around the generated PPM even in steady state. In fact, this is equivalent to the permanent search procedure of the PPM thus forcing the system to constantly oscillate around the PPM even if the latter is reached. These oscillations can be reduced by decreasing the value of the increment step D. However, a low value of D slows down the search for the PPM. Therefore, the choice of this step is a compromise between precision and speed which makes the tuning of this algorithm difficult.[25]

II. 2.2 Incrémental conductance algorithme (Inc) :

The disadvantage of the Perturb & Observe algorithm when tracking the peak power under fast varying atmospheric condition is overcome by the Incremental Conductance algorithm. The Incremental Conductance (Inc Cond) method is based on the fact that the slope dP/dv of the PV panel power-voltage curve is positive on the left side of the MPP, zero at the MPP, and negative on the right side of the MPP, as shown in **Figure (II.6)**

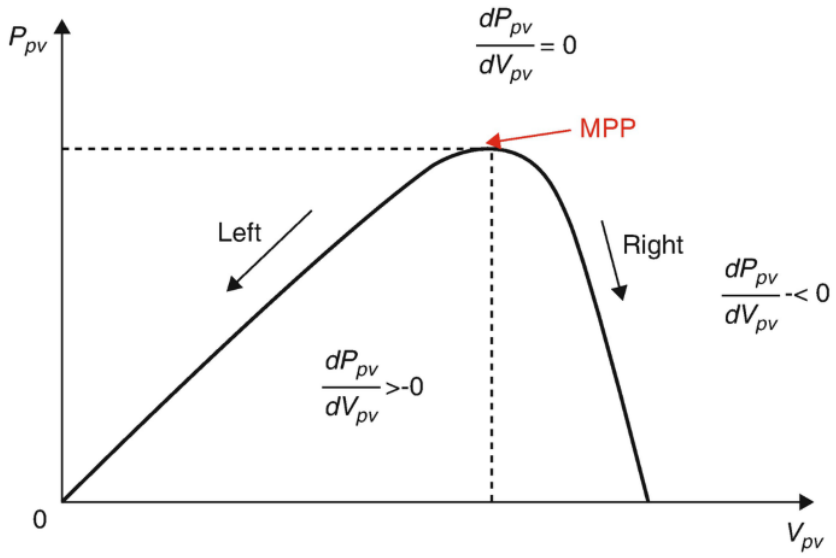

Figure II-6: principe de l'algorithme (Inc Cond)

The incremental and conductance algorithm makes use of the following equations:

At the MPP:

$$\frac{dP}{dV} = 0 \tag{II.3}$$

At the left of MPP:

$$\frac{dP}{dV} > 0 \tag{II.4}$$

At the right of MPP

$$\frac{dP}{dV} < 0 \;\; at\; the\; right\; of\; MPP \tag{II.5}$$

The abouve equations can be written in terms of voltage and current as follows:

$$\frac{dP}{dV} = \frac{d(V.I)}{dV} = I\frac{dV}{dV} + V\frac{dV}{dV} = I + V\frac{dI}{dV} \tag{II.6}$$

If the operating point is at the MPP equation **(II.6)** becomes:

$$I + V\frac{dI}{dV} = 0 \rightarrow \frac{dI}{dV} = -\frac{I}{V} \tag{II.7}$$

If the operating point is at the left side of the MPP equation (**II.6**) becomes:

$$I + V\frac{dI}{dV} > 0 \rightarrow \frac{dI}{dV} > -\frac{I}{V} \tag{II.8}$$

If the operating point is at the right side of the MPP equation (**II.6**), becomes:

$$I + V\frac{dI}{dV} < 0 \rightarrow \frac{dI}{dV} < -\frac{I}{V} \tag{II.9}$$

The flowchart shown in Figure (**II.7**) below describes the operation of this algorithm. It starts with measuring the present values of the PV generator voltage and current. Then, it calculates the incremental changes, dI and dV, using the present values and

algorithm is the increased complexity when compared to the Perturb and Observe algorithm.[26]

With:

$$\mathbf{e = I + V(\frac{\Delta Ipv}{\Delta Vpv})} \qquad \textbf{(II.10)}$$

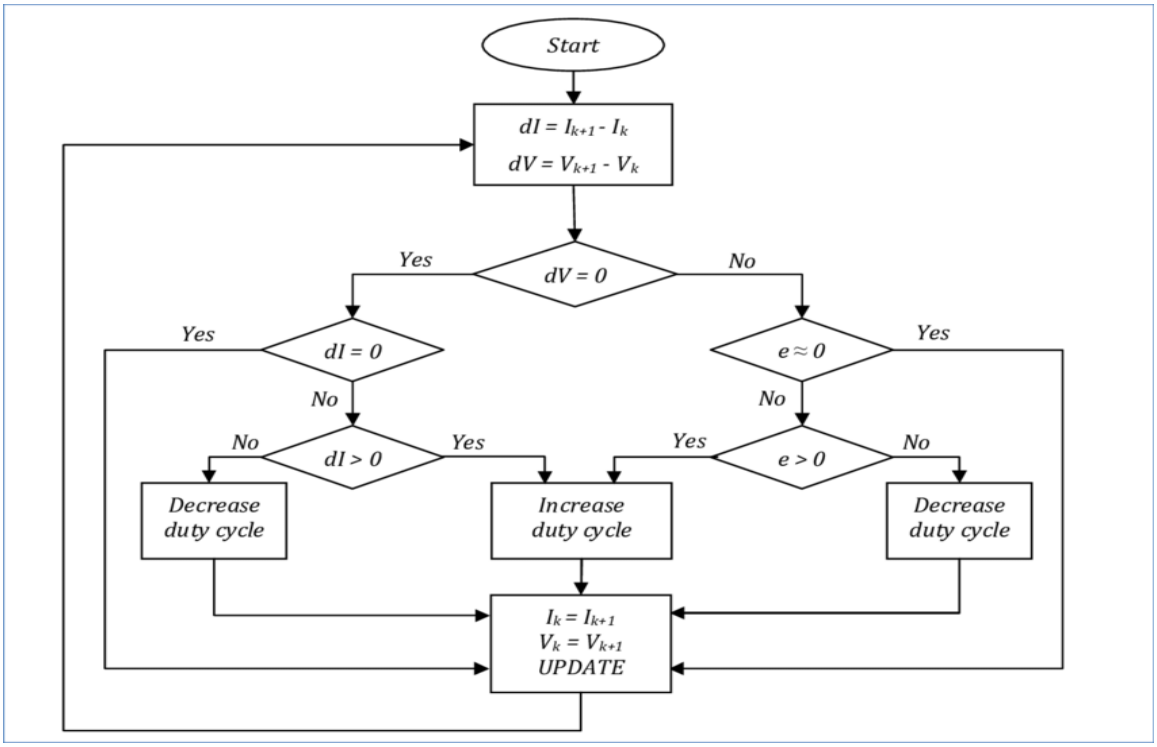

Figure II-7: flowchart algorithm (Inc Cond)

previous values of voltage and current. The main check is carried out using the relationships in the equations (II.7), (II.8), and (II.9). If the condition satisfies the inequality (II.9), it is assumed that the operating point is at the left side of the MPP therefore must be moved to the right by increasing the PVG voltage. Similarly, if the condition satisfies inequality (II.9), it is assumed that the operating point is at the right side of the MPP, thus must be moved to the left by decreasing the PVG voltage. When the operating point reaches the MPP, the condition satisfies the equation (II.9), and the algorithm bypasses the voltage adjustment. At the end of the cycle, it updates the history by storing the voltage and current data that will be used as previous values in the next cycle. Another important check included in this algorithm is to detect atmospheric conditions. If the MPPT is still operating at the MPP (condition: dV = 0) and the irradiation has not changed (condition: dI = 0), it takes no action. If the irradiation has increased (condition: dI > 0), it raises the MPP voltage. Then, the algorithm will increase the operating voltage to track the MPP. Similarly, in case of decreasing irradiation (condition: dI< 0), the MPP voltage will be lowered. Then, the algorithm will decrease the operating voltage. So it can be said that the incremental conductance can track rapidly increasing and decreasing irradiance conditions with higher accuracy than Perturb and Observe algorithm. One disadvantage of this

Advantages and Disadvantages (IncCond) MPPT Method:

Advantages :

- Accurate tracking of the Maximum Power Point (MPP).
- Effective under rapidly changing irradiance.
- Reduced oscillations around the MPP

Disadvantages:

- Higher algorithm complexity
- Slower response in low-power microcontrollers
- **Sensitive to measurement noise**

II.3 DC/DC photovoltaic converters

For power conversion, it is essential that efficiency is kept high to avoid power dissipation and to avoid excessive heating in electronic components. For this reason, all power conversion exchanged must be carried out around energy storage components (inductors and capacitors) and switches.

DC-DC converters used in PV systems are:

- Buck Converter ;
- Boost converter ;
- Buck-boost converter;

Thyristors have been generally used and accepted in the highest power levels.

Three converter topologies commonly used in photovoltaic systems are Buck and Boost and Buck-Boost as shown in Figure (II.8), to generate the desired voltages and currents. The Buck converter (Figure (II.9)), the Boost converter Figure (II.13) and the Buck-Boost converter Figure (II.14)

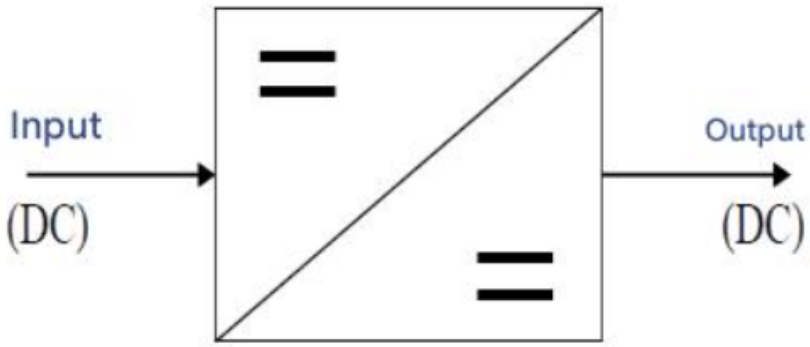

Figure II-8: Symbol of a DC-DC converter

This type of converter consists only of reactive elements (Self-contained, Capacitors) which, in the ideal case, do not consume any energy. This is why they are characterized by high efficiency.

In these studies, the converter switch is driven by a PWM (pulse width modulation) signal, with a fixed frequency fs and a variable duty cycle D.

Note that the power switches used depend on the level of power to be converted or controlled. MOSFETS (metal oxide field effect transistors) are usually used at

relatively low power (a few kW) and IGBTS (insulated gate bipolar transistors) at higher power.[27]

II.3.1 Buck Converter

The main role of the buck converter is to convert the input voltage to a lower output voltage. Figure (II.4) shows its ideal circuit :

Figure II-9 : Schéma de principe d'un convertisseur dévolteur (Buck)

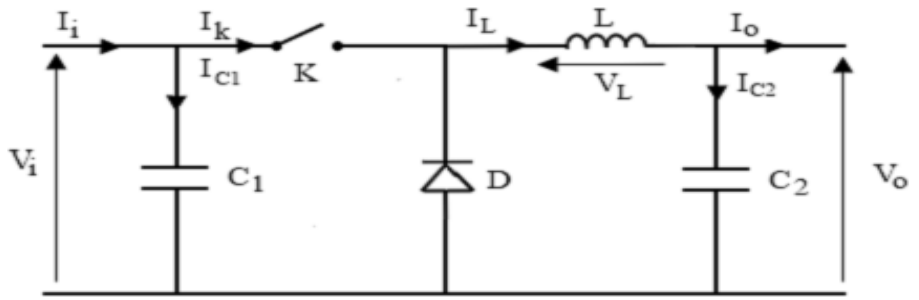

There are two operating cycles:

- ✓ During the closing time (t ∈ [0, D. Ts]), the diode blocks and a current flow in the load through the inductance, the latter then charges with energy.

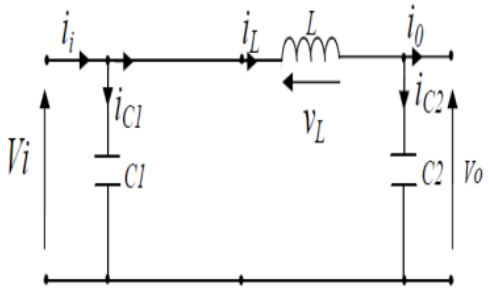

Figure II-10: Controlled transistor S is closed [0, D] Ts

- ✓ the switch opens (t ∈ [D. Ts, Ts]), the source and the load are no longer in contact, the diode saturates and the inductance releases energy to the load with a decrease in current.

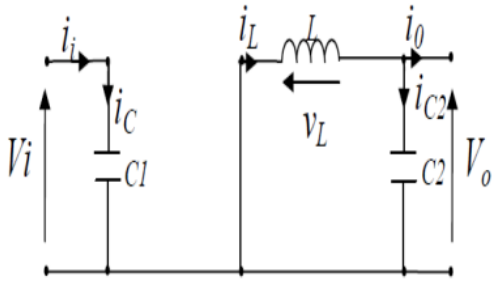

Figure II-11: the controlled transistor S is blocked [1 –D] Ts

The conversion ratio of a chopper is the ratio between the input voltage Vi and the output voltage Vo. For a step-down chopper, it is given in the following form:

$$V(D) = \frac{V_0}{V_i} = D \qquad \text{(II.11)}$$

So, the Buck converter is a voltage step-down.[28]

II.3.2 Boost converter

In this chopper, the average output voltage is higher than the input voltage, hence its name. This structure requires a switch with a controlled on and off (Bipolar, MOS, IGBT, etc.) and a diode (spontaneous on and off). The Boost converter is known as a voltage booster and, current step-down converter. Figure (II.12) represents the Boost electrical circuit.

This chopper has three components:

An inductor L, two capacitors C1, C2 and a switch K which can take two states, k=1 and k=0. During the operation of the chopper, the transistor will be switched at a constant frequency fs with a closing time [D.Ts]. During this time the current in the inductor increases gradually, as it stores energy, until the end of the first interval. And an opening time = [(1-D). Ts], The switch K opens and the inductor L delivers the current IL and thus generates a voltage which is added to the source voltage, which is applied to the load through the diode d. [29][30].

Or :

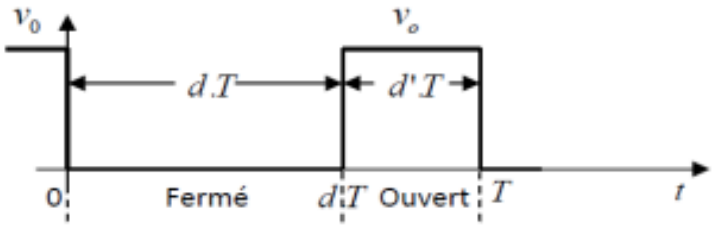

Figure II-12: closing and opening periods of a switch.

Ts: is the switching period which is equal to 1/fs.

D: the duty cycle of the switch (D∈ [0, 1]).

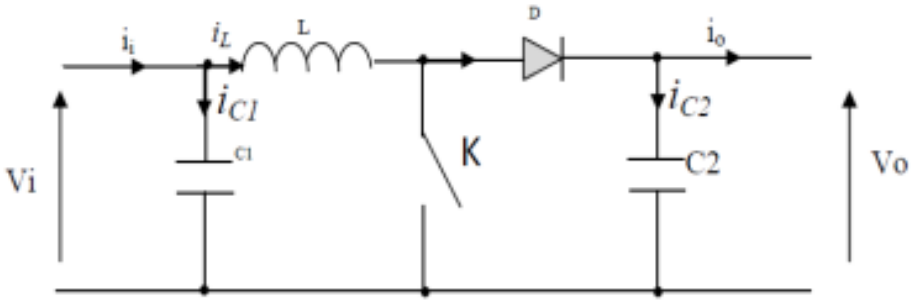

Figure II-13: Electrical diagram of the booster chopper

The main equation of the boost converter is:

$$\frac{V_0}{V_i} = \frac{I}{I-d} \qquad \text{(II.12)}$$

There are two operating cycles:

- ✓ During the first part of the operating cycle, from 0 to α.T, the controlled transistor S is closed (conducting). This time, the source and the load are not in contact during this phase. The diode is then blocked :

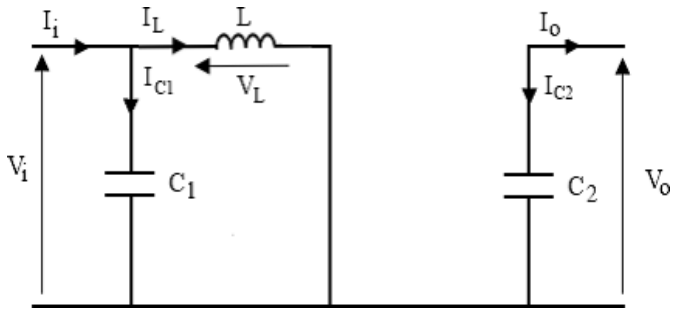

- ➢ (a): during the closing time (t ∈ [0, DTs]),

Figure II-14: the controlled transistor S is closed [0, D] Ts:

By applying Kirchhoff's laws, the electrical equations of current and voltage for the first period [0, D] Ts are:

$$\begin{cases} i_{c1} = C_1 \frac{d_{v_i}}{d_t} = i_i - i_L \\ i_{c2} = c2 \frac{d_{v0}}{d_t} = -i_0 \\ v_l = l \frac{di_l}{dt} = -V_i \end{cases} \qquad \text{(II.13)}$$

- ➢ In the second part of the cycle, from α.T to T, the controlled transistor S is opened and the diode becomes conductive. This is when the source and the load are connected. Its operating principle is based on the position of the open/closed switch S.

- ✓ (b): during the opening time (t ∈ [DTs, Ts]),

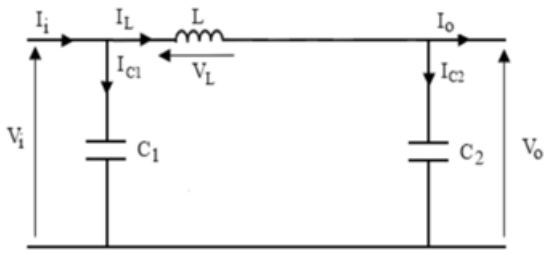

Figure II-15: controlled transistor S is blocked [1 – D] Ts

By applying Kirchhoff's laws, the electrical equations of current and voltage for the second period [1 – D] Ts are:[31]

$$\begin{cases} i_{c1} = c1\frac{d_{vi}}{d_t} = i_i \\ i_{c2} = c2\frac{d_{v0}}{d_t} = i_l - i_0 \\ v_l = l\frac{di_l}{dt} = v_{c1} * v_0 \end{cases} \quad \text{(II.14)}$$

II.3.3 Buck-boost converter

The latter has acquired the characteristics and electrical properties of the two types mentioned previously. It therefore presents a sort of hybrid transformer (step-down/step-up) for a continuous input/output voltage; its basic diagram is illustrated in figure (II.14)

The buck-boost converter combines the properties of the two previous converters, it is used as an ideal transformer from any input voltage to any desired output voltage; its basic diagram is shown in figure II16:

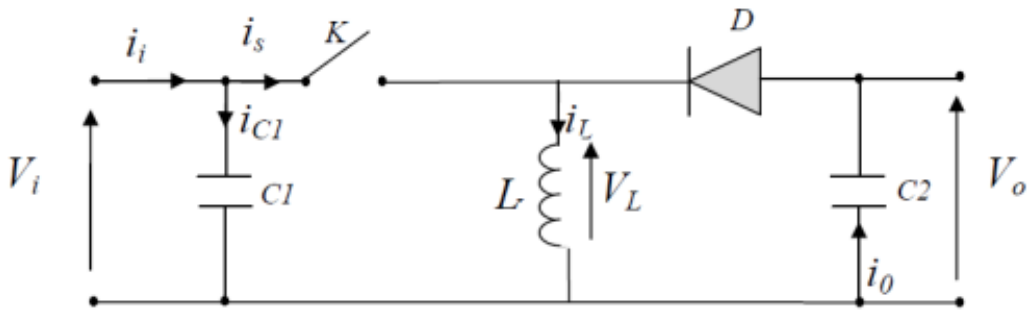

Figure II-16: Buck-Boost converter schematic diagram

- There are two operating cycles:

During the first part of the operating cycle, from 0 to DT, the controlled switch is closed (conducting). The diode is open and the inductor stores the energy supplied by the input generator.

- ✓ (a): during the closing time (t ∈ [0, DTs]),

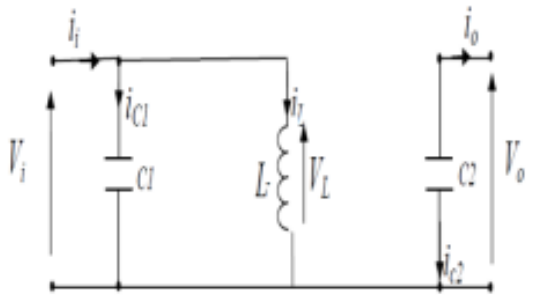

Figure II-17: Equivalent diagrams of the buck-boost chopper

- During the second part of the cycle, from α.T to T, the controlled switch is opened and the diode becomes conductive. The inductance restores its energy to the load.

It should be noted that the direction of the output voltage is reversed compared to the two previous cases.[32].

- ✓ (b): during the opening time (t ∈ [DTs, Ts]):

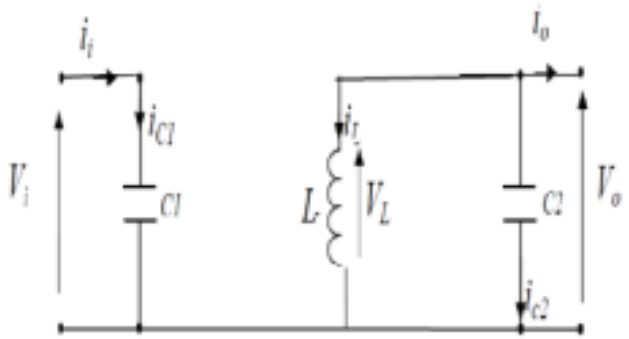

Figure II-18: Equivalent diagrams of the buck-boost chopper

Conclusion

In this chapter, we introduced the principle of maximum power point tracking. we also discussed some classic al maximum power point tracking (MPPT) algorithms, existing in the literature, these MPPT controllers are divided into two categories :indirect and direct types. Finally, we also presented the types of the DC/DC converters (boost, buck, and buck-boost).

In the next chapter, we will present the effect of irradiation and temperature on the electrical energy production in a photovoltaic installation, and will serve as a basis for comparing the two MPPT algorithms (P&O and INC cond).

Chapiter III:

Simulations and Results

Chapitre III: SIMULATIONS AND INTERPRETATIONS OF RESULTS

III.1. Introduction

In this chapter, we present the simulation results under the Matlab/Simulink environment (version 2017b) to carry out a comparative study of tracking the maximum power extracted from photovoltaic installation used two different classical algorithms.

The simulation system of this comparative study is composed of:

- A photovoltaic generator (PVG);
- A Boost converter with its control;
- Two types of MPPT algorithms of PVG such as:
  - ✓ Perturb & observe
  - ✓ Conductance increment

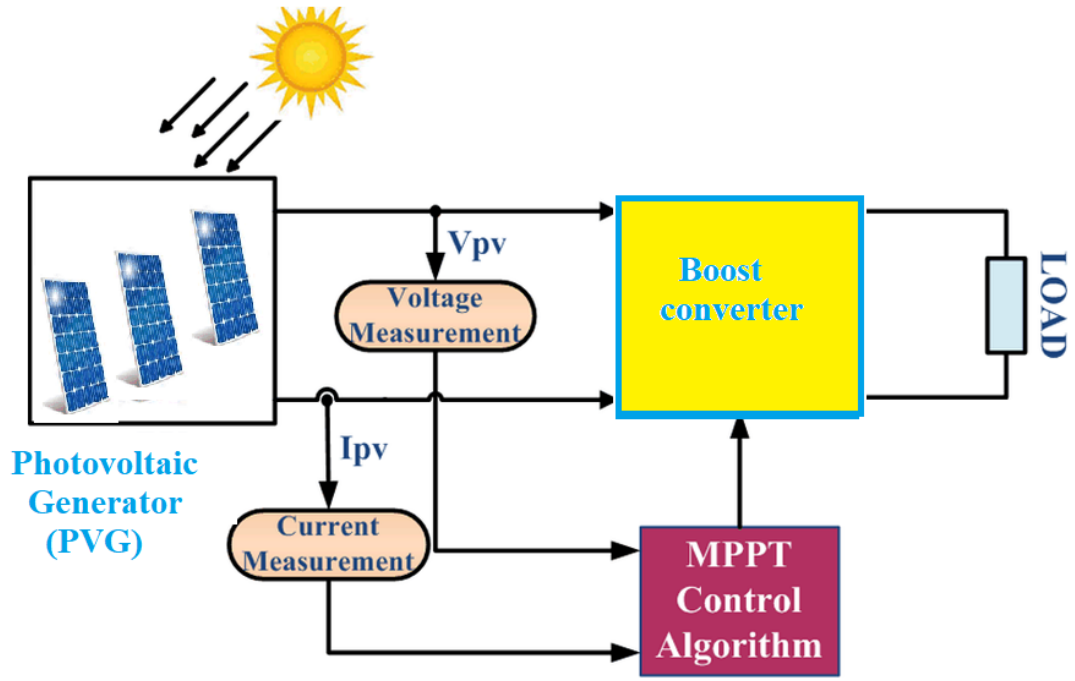

Figure III-1: General overview of photovoltaic generator MPPT controller

III.2. Characteristics of PV modules

The photovoltaic panel used in this simulation is Advanced Renewable Energy AREI-210W-M6-G [33] (see the appendix A). The characteristics power in function of voltage $P_{pv}(V_{pv})$ and current in function of voltage I_{pv} (V_{pv}) of used panel under optimal condition (G= 1000W/m2, T= 25C°) are presented in the Figure III.1.

Where:

The power at maximum point of this panel is P_{mpp}=210.4 W, its current at the maximum power point is I_{mpp} =7.2 A, its voltage at the maximum power point is V_{mpp}=29.22 V, open circuit voltage V_{oc}=36.6 and the short circuit current is I_{sc} =7.74 A.

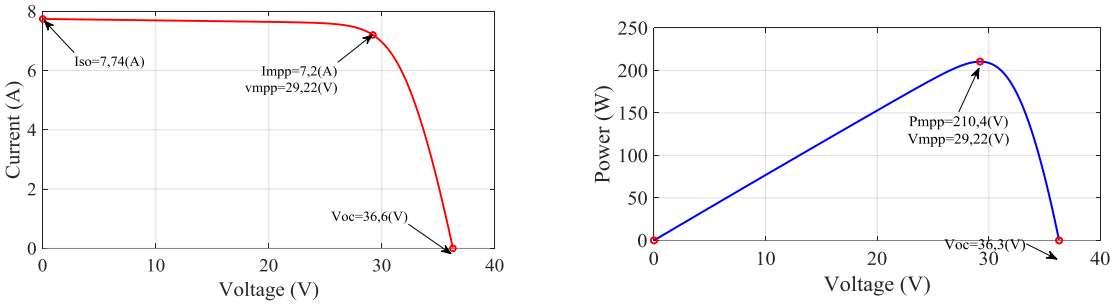

(a) Caractéristique I_{pv} =f(V_{pv}) (b) Caractéristique P_{pv} =f(Vpv)

Figure III-2: Characteristics of used photovoltaic panel.

III.3. Simulation results of photovoltaic generator

Figure (III.2) presents the simulation scheme of a PV generator that have:

1- Three series panels in raw and one string;
2- Boost converter with the following parameters: C_1= 950*10^{-6} F, C_2=300*10^{-6} F L= 4.8*10-3 H, R_L= 0.01 Ω;
3- Resistive load R=300 Ω;
4- MPPT controllers with duty cycle step Δd=0.05 with PWM=5000 Hz.

In this simulation, we take change the meteorological conditions such as the irradiation and temperature on the power produced by this generator and see the characteristics power in function of voltage $P_{pv}(V_{pv})$ and current in function of voltage $I(V_{pv})$ how they change under these conditions.

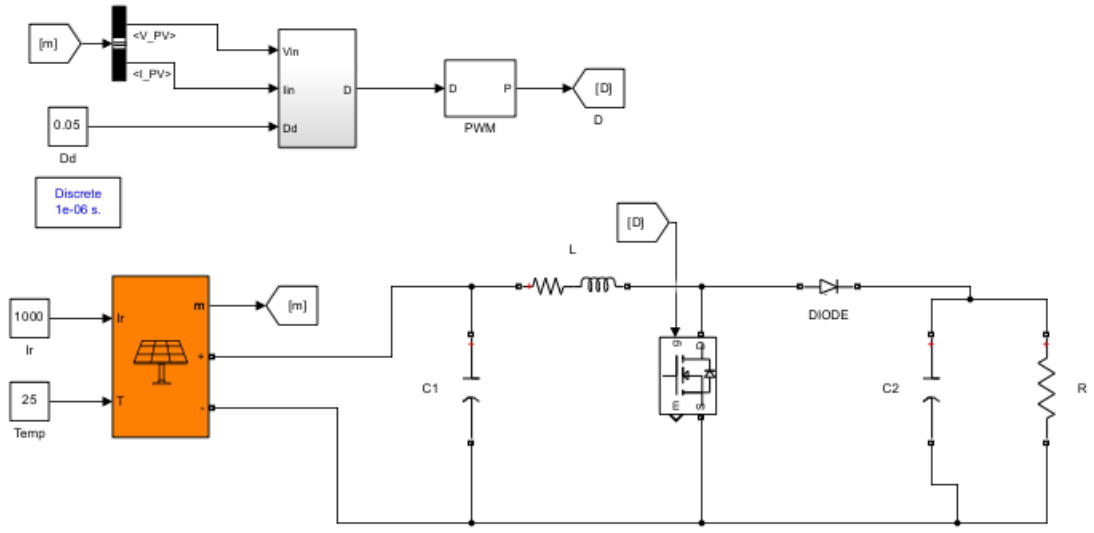

Figure III-3: Simulation scheme of the PVgenerator system

III.4. Influence of meteorological conditions on the characteristics PVG

The I_{pv} (V_{pv}) and P_{pv} (V_{pv}) characteristic is influenced by tow external meteorological conditions such as temperature degrees and irradiation intensities which act directly on the power peak of the PVG, the following figures show these influences

III.4.1. Influence of irradiation

Figure III.5 represents the influence of irradiation intensities on the characteristics of PV modules, at a constant temperature (25°C).

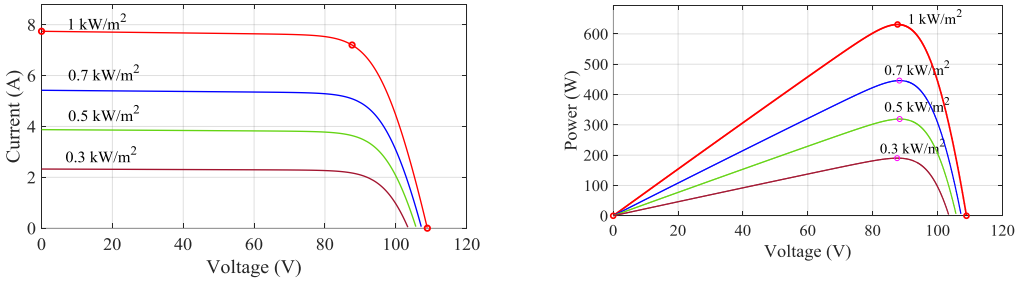

a. Characteristic $I_{pv}(V_{pv})$ b.Characteristic $P_{pv}(V_{pv})$

Figure III-4: Influence of irradiation intensities on PVG characteristics

From the characteristic I_{pv} (V_{pv}) in the Figure III.5, We note that the irradiation intensities variations cause a clear variation in current values which is proportional to this variation and a relatively small variation in voltage value on the characteristic I_{pv} (V_{pv}). And also, the characteristic P_{pv} (V_{pv}) changed with this variation. In which, the increased irradiation up the produced power by the PVG.

There is an important variation in maximum power produced under some irradiation intensities presented in the **table III.1**

TableIII. 1: Influence of Irradiation intensity variations on maximum power produced

Irradiation (kW/m^2)	Power (W)
1000	631.2
700	446.1
500	319.1
300	190.1

III.4.2 Influence of temperature

The temperature has an influence on the maximum power produced. The Figure III.6 shows this influence on the PVG characteristic.

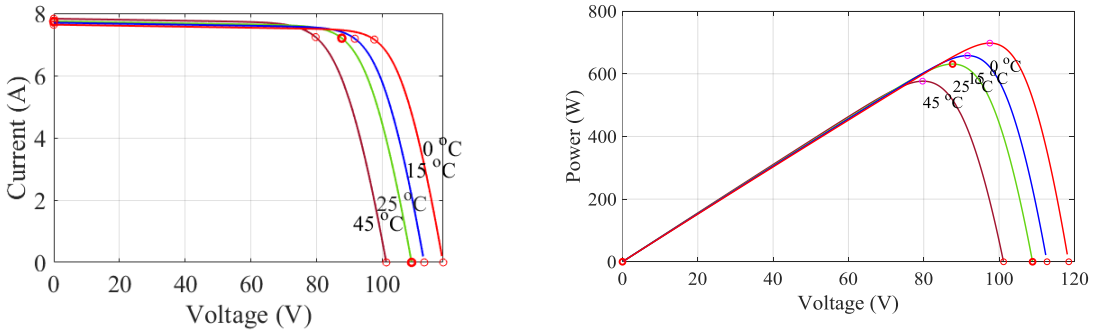

a. Characteristic $I_{pv}(V_{pv})$ b. Characteristic $P_{pv}(V_{pv})$

Figure III-5: Temperature influence on GPV characteristics.

It is noted that the current value change slightly with the temperature increases, but the temperature negatively affects the open circuit voltage. As the temperature increases, the open circuit voltage decreases. Therefore, the maximum power produced of the generator decreases.

Here same maximum power point produced by some temperature levels illustrated in the table IIIL 2.

TableIII. 2: Influence of temperature variations on maximum power produced

Temperature (°C)	Power (W)
0	697.9
15	658.1
25	631.2
45	576.4

III.5 Simulation results used different MPPT algorithms

In this phase, we used two MPPT algorithms such perturb and observe (P&O) and the second algorithm called incremental conductance (INC) under constant and variable meteorological conditions.

III.5.1. Simulation results under constant meteorological conditions

In this sub-phase, we present the simulation results of tow MPPT controls such as, P&O and INC made under constant meteorological conditions1000W/m^2 and temperature 25°C.

Figures III.6 shows a considerable oscillation at permanent regime in the voltage curves such as voltage curve of boost converter output (Vout) and the voltage curve of PVG Vpv)for the case of P&O control compared to Figure III.7 for the case of the INC control.

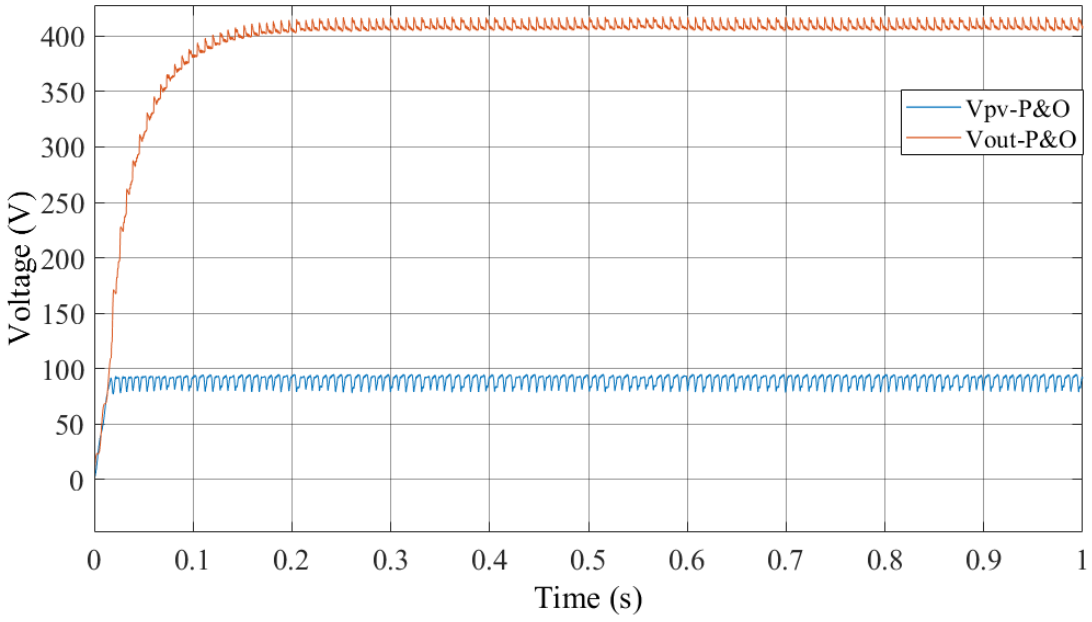

Figure III-6: Voltage curves using P&O control

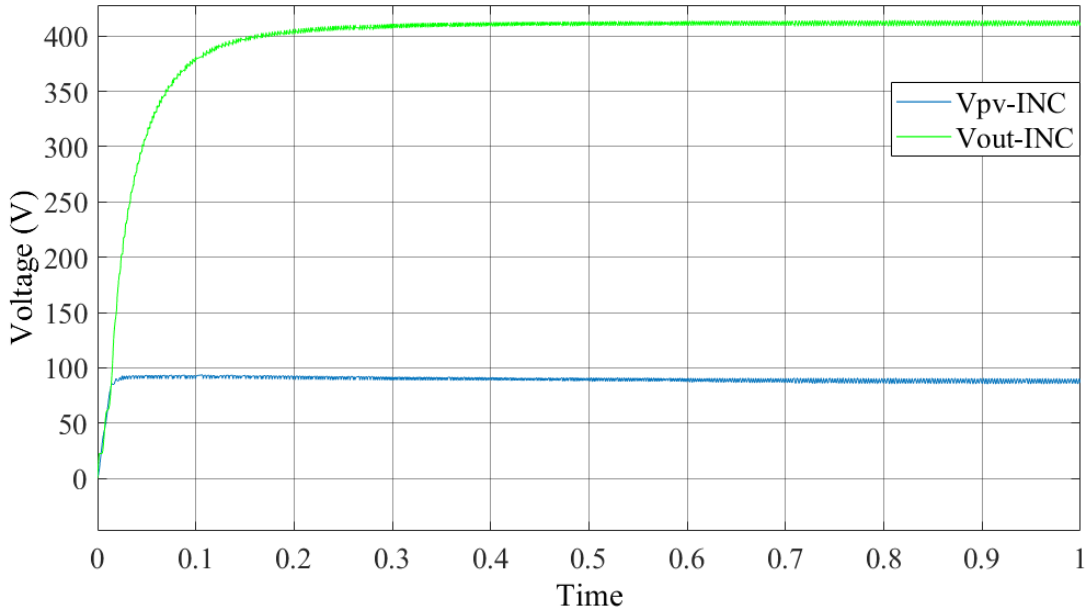

Figure III-7: Voltage curves using INC control

Figures III.14 shows a considerable oscillation at permanent regime in the current curves such as current curve of boost converter output (Iout) and the current curve of PVG (Ipv)for the case of P&O control compared to the Figure III.9 for the case of INC control see (Figure III.12).

.

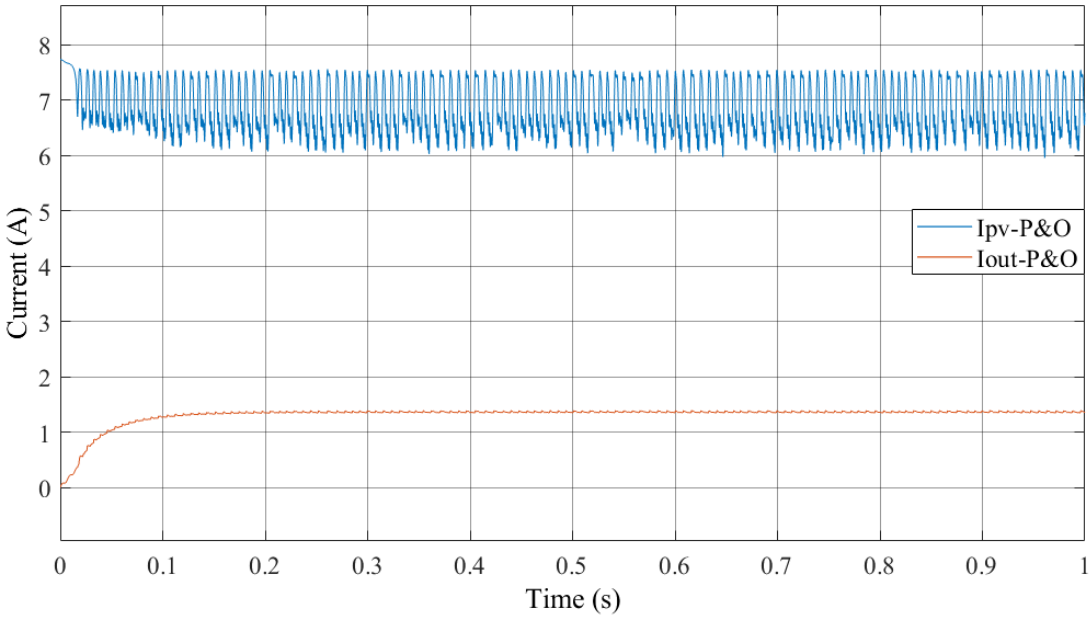

Figure III-8: Current curves using P&O control

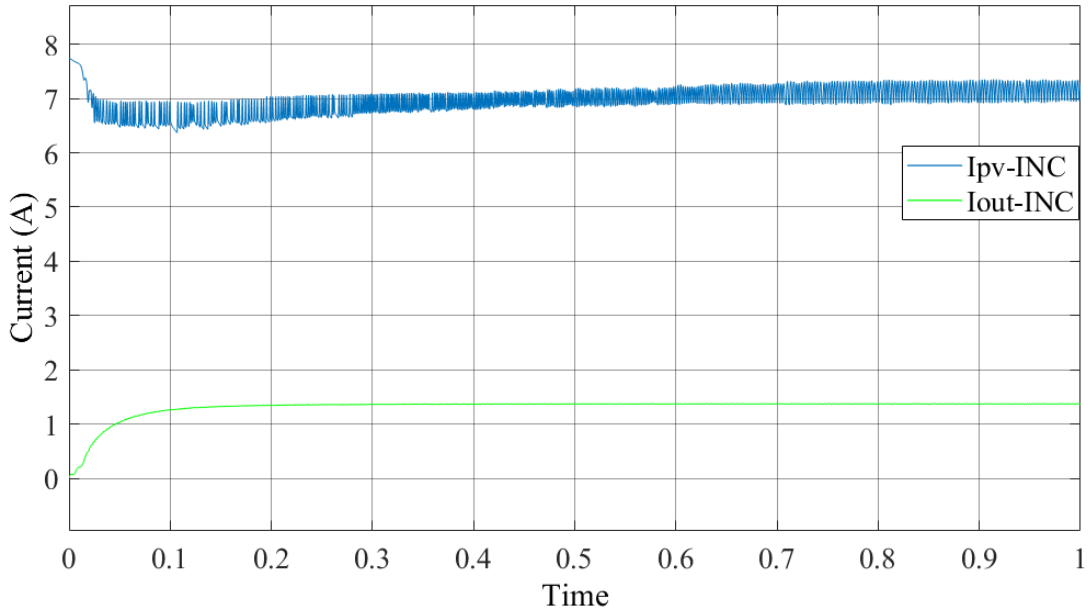

Figure III-9: Current curves using INC control

Figures III.11 shows a considerable oscillation at permanent regime in the power curves such as power curve of the boost converter output (Pout)and the power curve of PVG (Ppv) for case of P&O control compared to the power curves for the case of INC control see (Figure III.12).

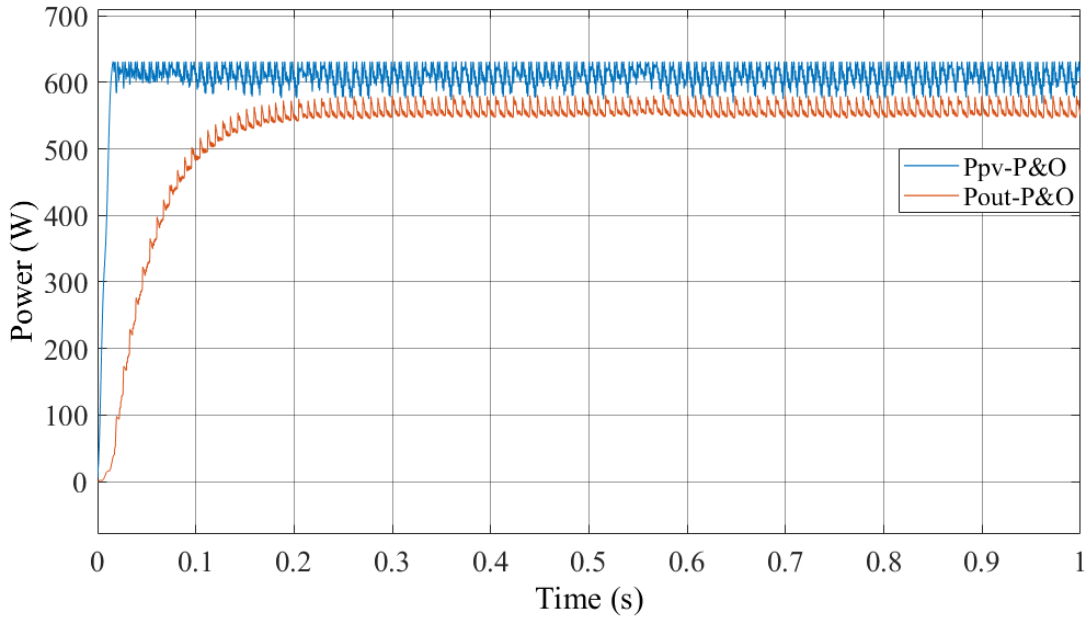

Figure III-10: Power curves using P&O control

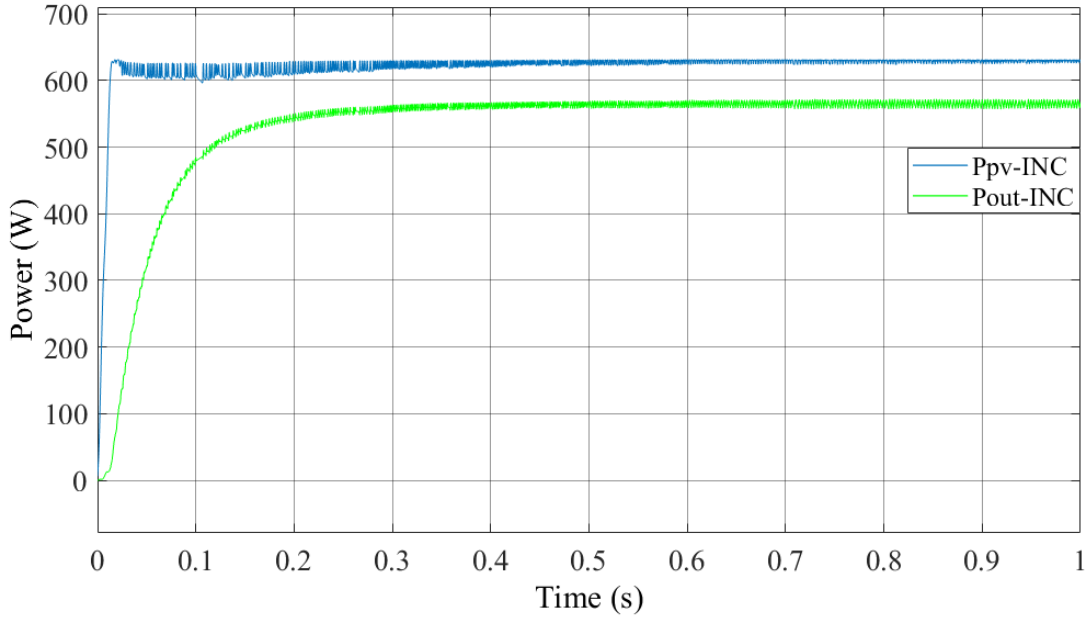

Figure III-11: Power curves using INC control

III.5.2 Simulation results under variable meteorological conditions

In this phase, we used two cases of meteorological variations such as:

- ✓ Progressive variations in temperature
- ✓ Sudden variation in irradiation with constant temperature.

a. Progressive variation in temperature

In this sub-phase, we change temperature progressively with constant irradiation as illustrate in the (Figure III.13)

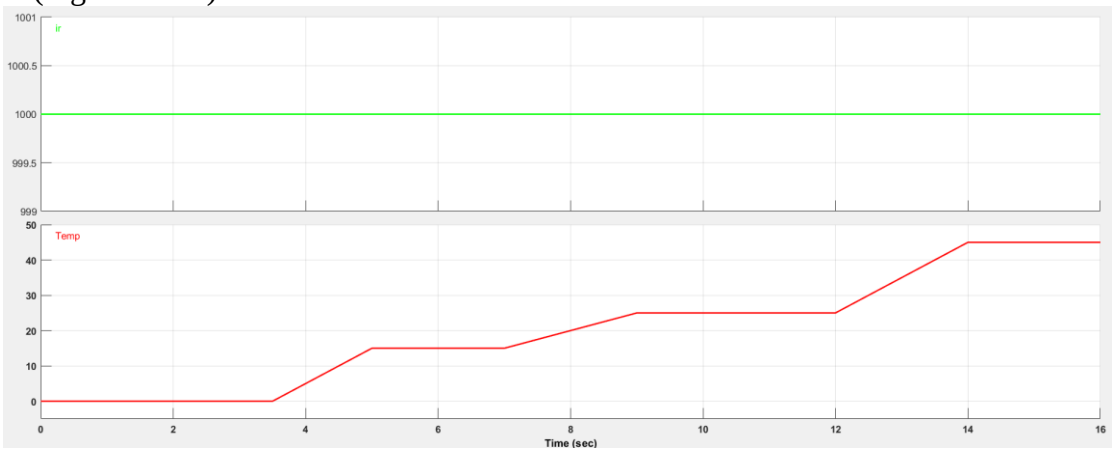

Figure III-12: Progressive variations in temperature with constant irradiation

In case of progressive variation in temperature with constant irradiation (1000 W/m2), the power produced by the boost converter (Pout-P&O) using P & O control follows the variation of produced power by PVG (Ppv-P&O) with the low difference between them depending to the variation of temperature level but with considerable oscillation level in two power curves see the (Figure III.14). The results are better when using the INC control see (Figure III.15). In this, the produced power by boot converter (Pout-INC) also follows the

produced power by PVG (Ppv-INC) with a low difference but it has a low level of oscillation compared to the case of the P&O control.

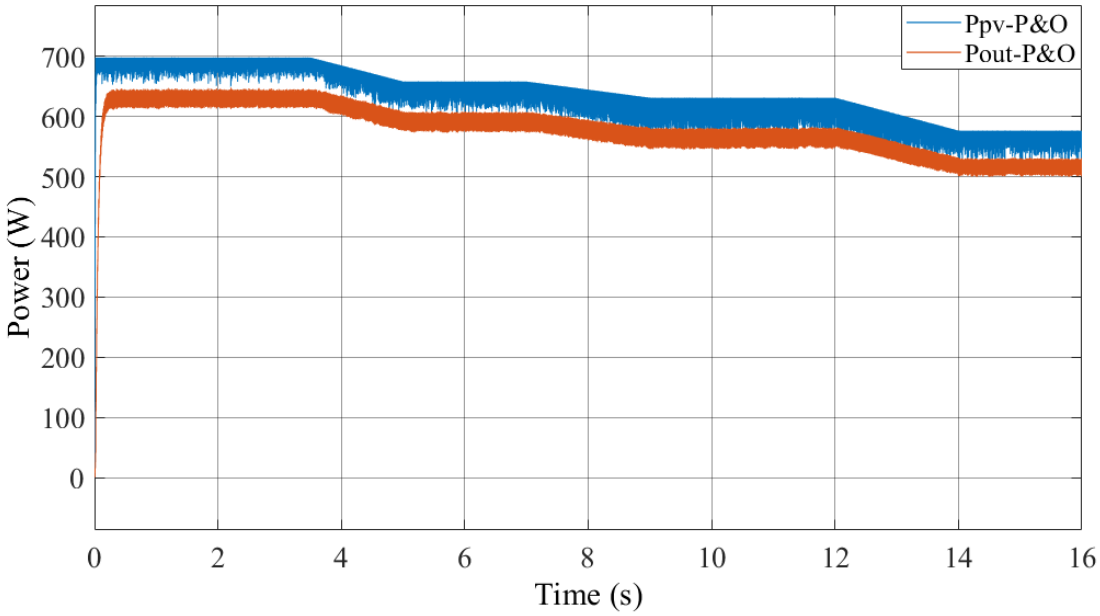

FigureIII-13: Power curves in case of progressive variations used P&O control

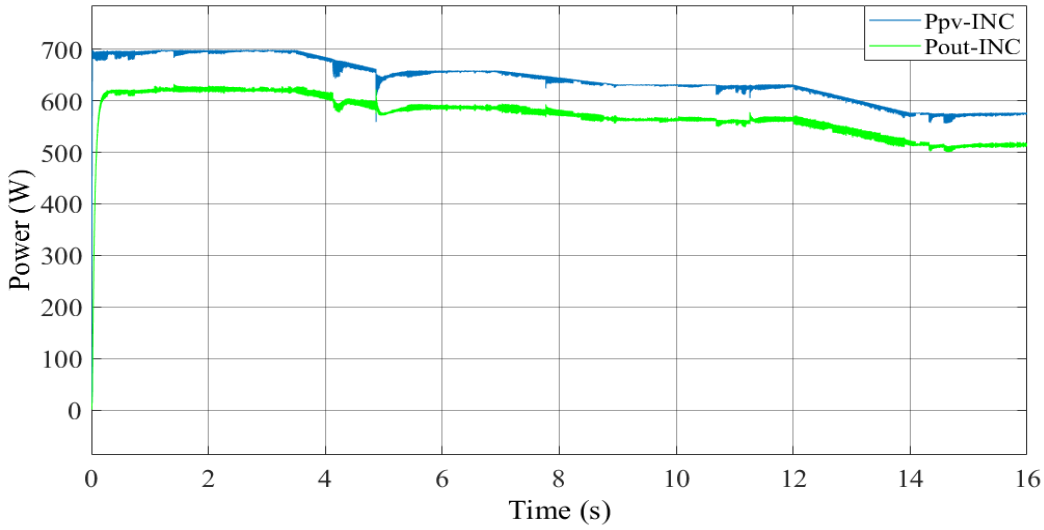

Figure III-14: Power curves in case of progressive variations used INC algorithm

a. Sudden variation in irradiation with constant temperature

We done here three sudden variations in value of irradiation with constant temperature as illustrate in the (Figure III.17):

1- From 1000 W/m^2 to 700 W/m^2
2- From 700 W/m^2 to 500 W/m^2
3- From 500 W/m^2 to 300 W/m^2

The main objective of this variation is to show the behavior of two MPPT controllers to follow this change.

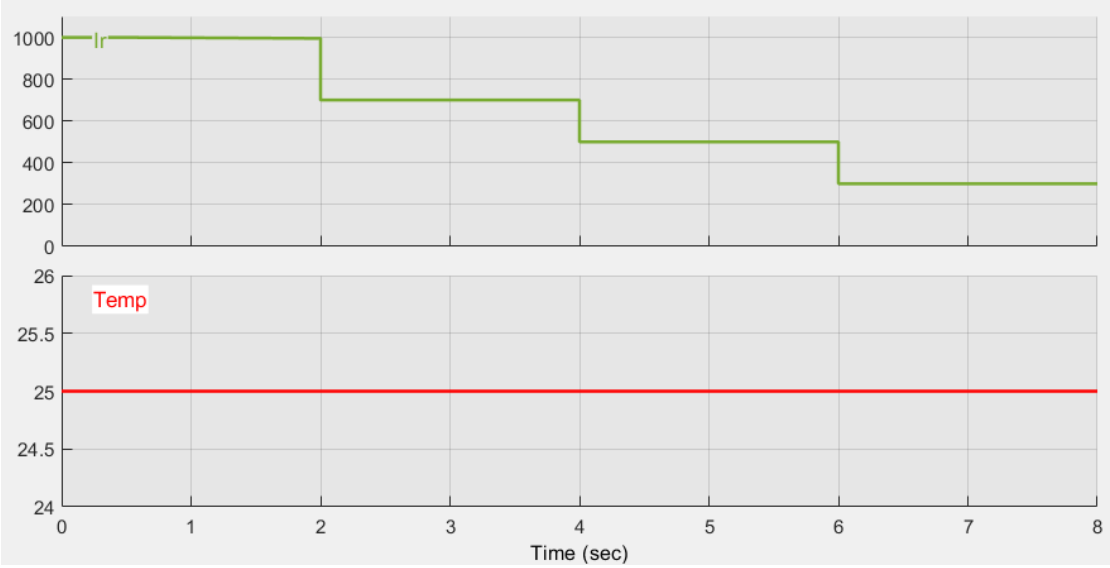

Figure III-15: Sudden variation in irradiation with constant temperature

In case of sudden variation in with constant temperature (temp =25 °C).the power produced by the boost converter (Pout-P&O) using P&O control follows the variation of produced power by PVG (Ppv-P&O) with the low difference between them depending to the variation of irradiation but here with different oscillation levels, where it is high in high irradiation (1000 W/m^2) then the oscillation level reduce when irradiation intensities decrease in two power curves (see the Figure III.17). The results are better when using the INC control (see Figure 3.18). In this, the produced power by boost converter (Pout-INC) also follows the produced power by PVG (Ppv-INC) with a low difference but it has a low level of oscillation compared to the case of the P&O control. The two algorithms here share the same inconvenient which they cannot immediately follow the sudden change in irradiation.

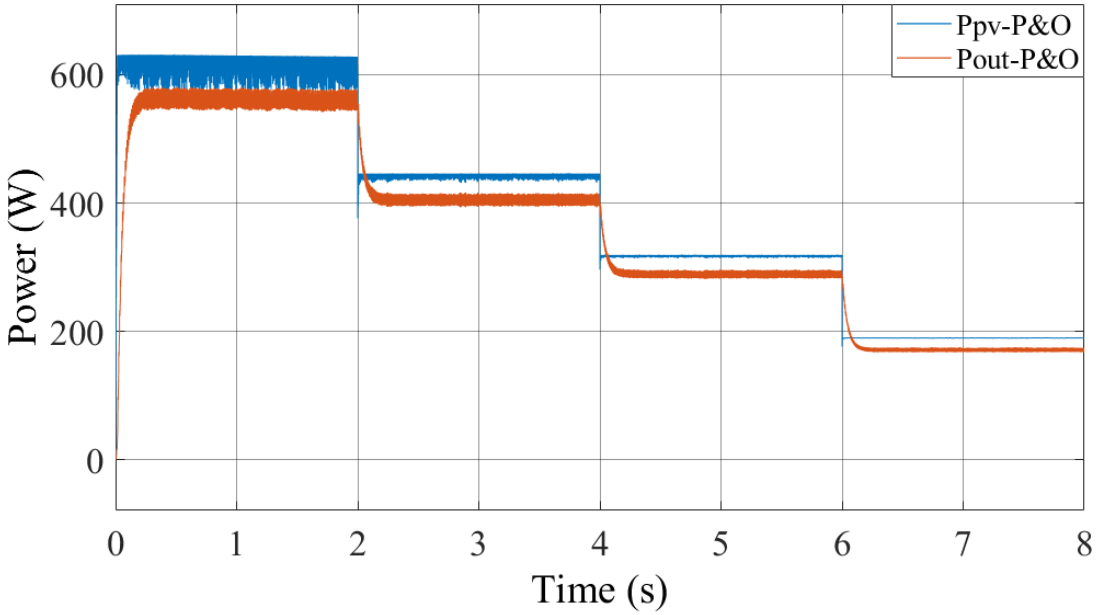

Figure III-16: Power curves in case of sudden variation used P&O algorithm

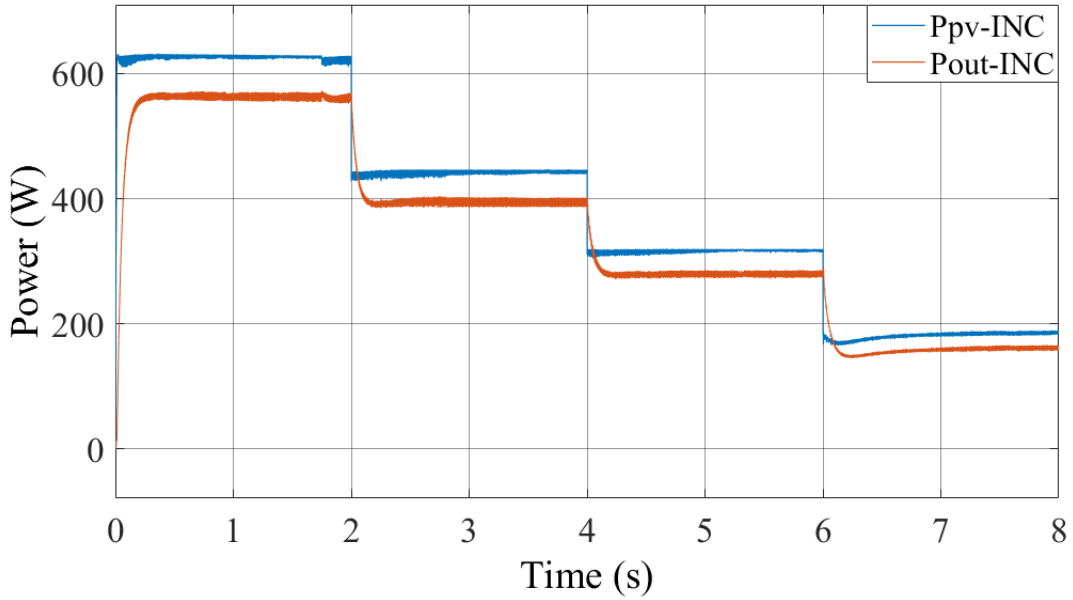

Figure III-17: Power curves in case of sudden variation using INC algorithm

The table III.3 present a comparative study of the obtained results between two MPPT controllers used in this study such as P&O and INC algorithms. From this table, the INC control present acceptable results in term of stability (low oscillation) and power produced by photovoltaic generator than two P&O control. However, in term of efficiency that it is here a little higher in case of P&O control than INC control. The same result fond in term of rapidity (transitional regime) for the two MPPT controls.

Table IIL3: comparative study of performance of the obtained results from two presented MPPT algorithms

In case of constant irradiation and temperature (ir=1000 W/m^2, temp= 25°C)		
	P&O algorithm	**INC algorithm**
Mean value	**Ppv –P&O= 606 W** **Pout –P&O = 527.53W**	**Ppv-INC= 617.8 W** **Pout-INC= 528.2 W**
Efficiency (%)	**87.05**	**85.5**
transitional regime	**T_{start} =0,3 s**	**T_{start} =0,3 s**
Oscillation level	**high**	**Low**
in case of progressive variation of temperature with constant irradiation (ir=1000 W/m^2)		
Mean value	**Ppv–P&O= 627.18 W** **Pout –P&O = 571.99W**	**Ppv-INC= 641.3672 W** **INC= 571.65 W**
Efficiency (%)	**91.2009**	**89.13**
transitional regime	**T_{start} =0,26 s**	**T_{start} =0,25 s**
Oscillation level	**High to low depending to the irradiation intensity**	**low**
in case of sudden variation in irradiation with constant temperature (temp=25°C)		
Mean value	**Ppv–P&O= 389.02 W** **Pout –P&O = 352.89W**	**Ppv-INC= 391.23 W** **Pout-INC= 346.12 W**
Efficiency (%)	**90.71**	**88.47**
transitional regime	**T_2=0,2 s**	**T_2=0,2 s**
Oscillation level	**High to low depending to the irradiation intensity**	**low**

III .6 Conclusion

In this chapter, a comparative simulation study between the different maximum power point tracking algorithms and the influence of irradiation and temperature has been presented. The different MPPT controls used are the conventional perturb and observe algorithm, the incremental conductance algorithm, this comparison is made in terms of rapidity, stability and efficiency.

Generaly, the INC control present acceptable result compared to P&O control.

General Conclusion

General Conclusion

In this work, we studied the modeling of a photovoltaic chain consisting of a photovoltaic generator, an adaptation stage (DC/DC Boost converter), a DC load (resistor), and a control stage to drive the converter (the classic MPPT control, in this case P&O, IncCond).

In this context, we presented renewable energy systems, paying particular attention to the photovoltaic system, which essentially consists of a photovoltaic generator (PVG) and a DC-DC Boost converter. The electrical model and mathematical equations of the Boost converter are explained. Various simulations, using the Matlab/Simulink environment, are performed to highlight the influence of variations in climatic conditions (illumination and temperature) on the MPP, where the system's operating power is at its maximum.

MPPT control, based on (P&O and IncCond) methods, provides the best connection between the photovoltaic generator (PVG) and the load, and forces it to always operate at its maximum power point. However, a comparative study of simulation results revealed that MPPT IncCond control provides better performance (reduced response time and error in steady-state operation) compared to P&O method.

With this work, we hope to contribute to the study of photovoltaic characteristics of solar cells, the study of stand-alone photovoltaic systems, and conventional MPPT controls.

As a future step in this work, it would be interesting to make an introduce more improvement to this work, study more MPPT techniques and implement the simulated MPPT techniques in hardware on microcontroller-based systems to validate the simulation results and confirm the performance obtained.

Reference

[1] Nzotcha, U., Kenfack, J., & Manjia, M. B. (2019). Integrated multicriteria decision making methodology for pumped hydroenergy storage plant site selection from a sustainable development perspective with an application. ***Renewable and Sustainable Energy Reviews, 112,*** **930–947.**

[2] AEI. (2016). ***World energy investment outlook | Special report*****. The International Energy Agency (IEA).**

[3] Kenfack, J., Bossou, O. V., Voufo, J., Djom, S., & Crettenand, N. (2016). New renewable energy promotion approach for rural electrification in Cameroon. In ***Renewable Energy in the Service of Mankind Vol II*** **(pp. 429–442). Springer, Cham.**

[4] Vitale, M., & Piazza, D. (2013). ***Photovoltaic sources: Modeling and emulation*****. Springer, Verlag London.**

[5] Hassan, M. M., Refat, K. H., Baten, M. Z., & Sajjad, R. N. ***Energy saving potential of...*** **[Note: Incomplète, veuillez fournir le titre complet.]**

[6] Knopf, H. (1999). ***Analysis, simulation, and evaluation of maximum power point tracking (MPPT) methods for a solar powered vehicle*** **(Master's thesis). Portland State University.**

[7] Gottschalg, R., Rommel, M., Ineld, D. G., & Ryssel, H. (1997). Comparison of different methods for the parameter determination of the solar cell's double exponential equation. In ***14th European Photovoltaic Science and Engineering Conference (PVSEC),*** **Barcelona, Spain.**

[8] ABB. (2010). ***Installation photovoltaïque, document technique*** **(p. 12). Italie.**

[9] Lerouge, C. (2006). ***Recherche & Industrie Photovoltaïque (PV) États-Unis*****. Sciences physiques, États-Unis.**

[10] Green, M. A., Emery, K., Hishikawa, Y., & Warta, W. (2008). Solar cell efficiency tables (Version 33). ***Progress in Photovoltaics: Research and Applications, 16,*** **61–67.**

[11] Pastor, M. A. C. (2006, September 29). ***Conception et réalisation de modules photovoltaïques électroniques*****.**

[12] Omar, A. M. E. H. (2012). ***Étude comparative entre différents modèles électriques photovoltaïques*****. Université Larbi Ben M'hidi, Oum El Bouaghi.**

[13] Kherchi, M. (2012). ***Conception et réalisation d'un caractériseur des modules photovoltaïques*** **(Mémoire de Magister). ENP.**

[14] Dida, M. (2021). ***Étude et amélioration des systèmes de conversion photovoltaïque dans les zones arides et semi-arides*****.**

[15] Bandou, F. (2013). ***Modélisation de modules photovoltaïques en milieu réel d'implantation*** **(Master professionnel). Université Mouloud Mammeri Tizi Ouzou.**

[16] Azizi, A. (2019). ***Modélisation et optimisation d'un système de production d'énergie photovoltaïque avec un système de stockage hybride*** **(Thèse de doctorat). Université Badji Mokhtar - Annaba.**

[17] Khenfer, R. (2015). ***Détection et isolation de défauts combinant des méthodes à base de données appliquées aux systèmes électro-énergétiques*** **(Thèse de doctorat). Université Ferhat Abbès - Sétif.**

[18] Hachana, O. (2015, June 6). ***Étude d'un système photovoltaïque en vue du diagnostic*** **(Thèse de doctorat 3e cycle, LMD).**

[19] Benadel, F. (2016). ***Étude et simulation d'une commande MPPT pour système PV*** **(Mémoire de Master académique). Université Mohamed Boudiaf - M'Sila.**

[20] Cabal, C. (2008). ***Optimisation énergétique de l'étage d'adaptation électronique dédié à la conversion photovoltaïque*** **(Thèse de doctorat). Université de Toulouse.**

[21] Boulhares, I. (2020). ***Étude comparative des performances de différentes commandes MPPT*** **(Master académique). Université Ahmed Draïa - Adrar.**

[22] (Doublon avec 19) Benadel, F. (2016). ***Étude et simulation d'une commande MPPT pour système PV*** **(Mémoire de Master académique). Université Mohamed Boudiaf - M'Sila.**

[23] Ressources naturelles du Canada. (2018). ***Les systèmes photovoltaïques (guide de l'acheteur)*****. Division de l'énergie renouvelable et électrique. Ottawa, Canada.**

[24] Motahhir, S., El Ghzizal, A., & Derouich, A. (2015). Modélisation et commande d'un panneau photovoltaïque dans l'environnement PSIM. ***CIGIMS 2015*****, EST de Fès.**

[25]Aamarouayache, M. (2014). ***Contribution à l'optimisation d'une chaîne de conversion d'énergie photovoltaïque*** **(Doctorat en sciences en électrotechnique).**

[26] Malki, S. (2001). ***Maximum Power Point Tracking (MPPT) for Photovoltaic Systems*** **(Mémoire de Magister). Université Mohamed Bougara Boumerdes.**

[27] Université Sétif 1. (2013). ***Optimisation de la poursuite du point de puissance maximale (MPPT) d'un système photovoltaïque par les techniques intelligentes*** **(Mémoire de Magister en Electrotechnique).**

[28] Université Mohamed Boudiaf - M'Sila. (2019). ***Amélioration de la commande MPPT d'un système photovoltaïque par backstepping*** **(Master académique).**

[29] Lasmi, Y. (2013). ***Optimisation de la poursuite du point de puissance maximale (MPPT) d'un système photovoltaïque par les techniques intelligentes*** **(Mémoire de Magister). Université Sétif 1.**

[30] Moulay-Amar, M., & Loghouini, M. (2005). ***Étude et réalisation d'un système de poursuite de point de puissance maximale à base de microcontrôleur destiné à une installation photovoltaïque*** **(Mémoire d'ingéniorat). Université de Ouargla, Algérie.**

[31] Benseddik, O., & Djaloud, F. (2012, June 27). ***Étude et optimisation du fonctionnement d'un système photovoltaïque*** **(Mémoire de Master). Université Kasdi Merbah - Ouargla.**

[32] École nationale polytechnique. (2011). ***Étude et simulation des systèmes photovoltaïques avec micro-convertisseurs*** **(Mémoire de Magister).**

[33] EnergyPal. (s.d.). ***Best solar panels for homes: Alpha Solar Planet ASP210M6-48.***
https://www.solarhub.com/product-catalog/pv-modules/3-AREi-210W-M6-G-Advanced-Renewable-Energy

appendix

Module: Advanced Renewable Energy AREi-210W-M6-G

PV Module AREi-210W-M6-G Details

Manufacturer: Advanced Renewable Energy
Model Number: AREi-210W-M6-G
Production Status: unknown
CSI Approved: Yes
CSI Model Number: AREi-210W-M6-G
Description: 210W Polycrystalline Module

Electrical parameter

Power at STC (W)	210
Power at PTC (W)	187.4
Bifacial	No
Bifaciality (%)	-
Lower Power Tolerance (%)	-
Upper Power Tolerance (%)	-
Power Density at STC (W / m2)	129.63
Power Density at PTC (W / m2)	115.679
Module Efficiency (%)	-
Cell Efficiency (%)	-
Vmp: Voltage at Max Power (V)	29.22
Imp: Current at Max Power (A)	7.2
Voc: Open Circuit Voltage (V)	36.3
Isc: Short Circuit Current (A)	7.74
Max System Voltage (V)	-
Series Fuse Rating (A)	-
Bypass Diode	-
Nominal Operating Cell Temp (°C)	44.5
Open Circuit Voltage Temp Coefficient (% / °C)	-0.353
Short Circuit Current Temp Coefficient (% / °C)	0.055

Max Power Temp Coefficient (% / °C)	-0.507

Mechanical parameter

Cell Type	Poly
Connector Type	-
Connector Cable Length (mm)	-
Length (mm)	1637.0
Width (mm)	987.0
Module area (m2)	1.62
Depth (mm)	-
Weight (kg)	-
Bipv	No
Frame Color	-
Backsheet Color	-